Power Forecasting-Based Coordination Dispatch of PV Power Generation and Electric Vehicles Charging in Microgrid

Ying Hao[1], Lei Dong[1], Jun Liang[2], Xiaozhong Liao[1], Lijie Wang[3], Lefeng Shi[4]

[1]Department of Automation, Beijing Institute of Technology, China

[2]School of Engineering, Cardiff University, UK

[3]Department of Electrical Engineering, Beijing Information Science and Technology University, China

[4]School of Economics and Management, Center for Intelligent Energy Management and Applications, Chongqing Normal University, China

Abstract: We propose herein an extended power forecasting-based coordination dispatch method for PV power generation microgrid with plug-in EVs (PVEVM) to improve the local consumption of renewable energy in the microgrid by guiding electric vehicle (EV) orderly charging. In this method, we use a clustering algorithm and neural network to build a power forecasting model (PFM) based on real data which can effectively characterise the uncertainty of PV power generation and EV charging load. Based on the interaction between the energy control centre (ECC) of the PVEVM and the EV users, a one-leader multiple-follower Stackelberg game is formulated, and the Stackelberg equilibrium is determined by using a power forecasting-based genetic algorithm (GA). As a main contribution of this paper, the PV power generation and EV charging load output from the PFM are used to generate a better quality initial population of the GA to improve its performance. A case study using real data from the Aifeisheng PV power station in China and EV charging stations in the UK verifies the good performance of the proposed extended coordination dispatch algorithm.

Keywords: Power forecasting model; Electric vehicle orderly charging; Stackelberg game; Local consumption of renewable energy; Initial population of genetic algorithm

1. Introduction

A microgrid is an important part of the smart grid, which plays an essential role in improving the distributed renewable energy consumption and ensuring the power supply reliability. Moreover, because of the developments in renewable energy, the promotions of the reform in the electricity market, and the maturity of the energy management technology, an increasing number of microgrids are expected to be included in the distribution system. However, as the renewable energy resources (such as wind and solar energy) are inherently volatile [1], their output power is always fluctuating and uncertain, which severely hinders their advancement. At the same time, electric vehicles (EVs) are also greatly challenged by the randomness of their disordered charging, which may lower the grid reliability [2].

However, the EVs (as a distributed storage system that is easy to guide and plan) can be plugged into the microgrid as a flexible load to participate in energy management; this could alleviate the adverse impact caused to the grid when the EV charging process and renewable energy system are separately operated. Because of the uncertainty of the renewable energy and the randomness of the EV charging behaviour, coordination of the EV charging with other grid load and renewable energy generation has become a challenge [3]. In this context, the existing related research works are divided into three main categories, based on their objectives: energy utilisation, costaware, and the impact on the grid.

(1) *Energy utilisation*: This research category focuses on improving the efficiency and utilisation of renewable energy. For instance, Zhou et al. [4] proposed the use of EVs as a responsive demand to relieve the network stress caused by generation curtailment. This is achieved by guiding the EVs to absorb the excessive renewable energy generation. They used a 47-node network to quantitatively analyse the resulting benefits and reported that the combined management strategy could achieve 7.9% improvement in the utilisation of renewable energy. Similarly, Hou et al. [5] maximised the utilization renewable energy and minimised the integrated operation cost by using energy storage and controllable EVs. To verify the effectiveness of their proposed strategy, they compared their results with that of a random charging operation of the EVs.

(2) *Costaware*: This research category focuses not only on reducing the cost of operation, electricity generation, and EV charging, but also on increasing profit for the service providers. For instance, Shen, and Cui [6] simulated a power system with EVs and renewable energy sources (RESs) based on the data collected from Melbourne and demonstrated that the integration of the EVs and RESs into the power system can reduce the cost and emission of electricity by intelligently guiding the charging/discharging of the EVs. Zhao et al. [7] developed a novel economic dispatch model, which can minimise the generation cost by considering the uncertainties of the EVs and wind power generation. Chen and Duan [8] presented a method for the optimal integration of the EVs into the microgrid using a PV solar power system, which considered the optimal parking numbers under optimal scheduling of the EVs and aimed at minimising the total cost of the microgrid. In [3], the EVs were used as a flexible demand for the active network management to increase the investment benefits from the demand side management perspective. Ju et al. [9] proposed a multi-objective optimisation model for a virtual power plant (VPP) using wind power generation, PV power generation, and EVs. The objective of this multi-objective optimisation model was to minimise the system compensation and abandoned energy costs, and maximise VPP operation income, which was verified by an actual distributed power demonstration project.

(3) *Impact on the grid*: These research works discuss how to alleviate the adverse impact on the grid. Yuan et al. [10] established an economic optimal dispatch VPP model with renewable energy generation and EVs to reduce the adverse impact on the grid due to the separate operation of the EV

charging and renewable energy. They designed an economical operation strategy for VPP with EVs to not only compensate for the renewable energy generation deviation, but also to reduce the spinning reserve capacity and improve the reliability of the VPP. Li et al. [11] built an optimal operation model of a PV-assisted charging station, which could effectively control the charging cost and reduce the off-peak load difference, by considering the charging cost and charge/discharge cycle number of the energy storage system as the objective function.

Therefore, combining the EV orderly charging and renewable energy using a coordination dispatch model is a possible approach towards improving the local renewable energy consumption, increasing profit for the participants, and reducing the load fluctuations in the distribution network caused by the plug-in EVs [3, 12, 13]. There are two main control methods for EV orderly charging: direct charging load control and charging price incentive control [14]. The former directly controls the EV user's charging behaviour through the order issued by the charging dispatch centre according to the load condition of the grid, while the latter encourages the EV user to independently participate in the orderly charging according to the electricity price—this method can enable the timely transfer of the charging load while the EV user seeks the lowest charging cost. The increasingly mature energy trading market enables wider usage of this method as an EV orderly charging control strategy [15-18]. Many studies have been conducted on the electricity price-based charging strategy for renewable energy-powered EV charging stations. Mingrui et al. [19] developed a pricing incentive mechanism to manage EV charging according to the typical daily wind power and PV power generation and the load in the microgrid. Qifeng et al. [20] proposed real-time pricing based on an automatic demand response strategy for PV-powered EV charging stations (PVCSs) to minimise the cost of electricity purchased from the grid. Yeong et al. [21] developed a profit-optimal management strategy based on the Lyapunov optimal algorithm by controlling the price of charging services and the number of EVs to increase the profit of charging stations. Xiaodong et al. [22] applied a model predictive control method to realise dynamic interactive response control for EVs.

However, unlike in the traditional optimisation problems, the charging station operator would expect a high retail electricity price. Because the daily average retail electricity price must be fixed, and as the price fluctuates above and below the average [23], the EV users would inevitably choose to charge during the low-price period. Therefore, there is an interactive competition between the operator and EV users: the Stackelberg game is usually considered to characterise the decision-making strategies of the operator and EV users in the coordination dispatch. Wang et al. [24] proposed a charging scheme based on a four-stage Stackelberg game for EVs in a smart community with renewable energy resources. Zhang et al. [25] proposed and analysed a hierarchically distributed energy management for the PVCSs. They achieved a cooperative and generalised Stackelberg equilibrium at the station and EV levels through a two-level distribution game. Rui et al. [26] designed a day-ahead price model based on the Stackelberg game model for the PVCS. They established a day-ahead price strategy based on a PV power generation forecasting model and analysed the impact of the accuracy of PV power generation forecast on the profit of the PVCS operator.

The objective of the Stackelberg game in the coordination dispatch is to determine the Stackelberg equilibrium point, in addition to establishing the game model. At the Stackelberg equilibrium, neither the leader nor any follower can benefit in terms of either total cost or utility, respectively, by unilaterally changing strategies [27]. When the corresponding strategy set is relatively abundant in the Stackelberg game, the traditional cyclic search method is inefficient and cannot adapt to the demand of the actual solution. Many studies consider finding the Stackelberg equilibrium as an optimisation problem, which can be solved by using techniques such as genetic algorithm (GA) [8, 28], particle swarm optimisation (PSO) [29], differential evolution (DE) [26], or Karush–Kuhn–Tucker conditions [30]. Among these, the GA, PSO, and DE are metaheuristic optimisation algorithms: essentially, these begin by randomly generating an initial population; then, they iteratively calculate through the

selection, crossover, and mutation operations according to a certain principle [31]. Among these techniques, GA is the most popular. However, despite producing good results, many studies have focused on ways to improve its performance, such as generating an initial population of better quality [32, 33]. This is because the operations in the GA, such as selection, crossover, and mutation, are all based on the initial population; hence, the quality of the initial population is very important—a better initial population can adjust the search range of the algorithm to avoid some problems caused by population diversity.

According to the current research above, there is an optimisation problem in the coordination dispatch of renewable energy generation and EV charging, because both the renewable energy-powered EV charging station operator and EV users expect high profit. However, unlike the traditional optimisation problems, there is an interplay between the charging station operator and EV users during the energy trading process. The Stackelberg game is usually used to design their behaviour, in which charging station operator is the leader of the game, and EV users are the followers. In addition to establishing the Stackelberg game model for the coordination dispatch, how to determine the Stackelberg equilibrium point is one of the technically difficult problems to be solved in this research field. Many studies solved this problem by using GA. However, as a metaheuristic optimisation algorithm, some studies have shown that the GA algorithm itself can be further improved. Therefore, an improved GA based on the characteristics of PV power generation and EV charging could improve its performance to achieve the Stackelberg equilibrium in the coordination dispatch model. To the best of our knowledge, no published literature on the coordination dispatch that has used the Stackelberg game mentioned above, has considered the initial population of the optimisation algorithm.

Therefore, this paper proposes an extended coordination dispatch algorithm based on the Stackelberg game which is solved by an improved power forecasting-based GA. This extended coordination dispatch algorithm considers not only the local consumption of PV power generation, but also the uncertainty of PV power generation and EV charging load using a power forecasting model (PFM) based on clustering algorithm and neural network. Firstly, we study the energy trading model of the PV power generation microgrid with plug-in EVs (PVEVM) in the wholesale market, the EV charging cost function considering the dissatisfaction cost and the energy trading strategy between the energy control centre (ECC) of the PVEVM and the EV users. Then, we formulate a one-leader multiple-follower Stackelberg game, and solve the Stackelberg equilibrium via an improved power forecasting-based GA. Furthermore, the specific initial population of the improved GA, which is generated by the PV power generation and EV charging load day-ahead forecasted data from PFM using the real data, reduces the boundary of the initial population, generates a more reasonable initial population, which in turn improves the performance of the GA in solving the Stackelberg game for the coordination dispatch. The validity and efficiency of the proposed extended coordination dispatch algorithm were evaluated using real data obtained from the Aifeisheng PV power station in China and EV charging stations in the UK.

The remainder of this paper is organised as follows: Section 2 presents a mathematical description of the PVEVM energy trading model, the EV charging cost function considering the dissatisfaction cost, and the formulation of the energy trading process. Section 3 outlines the extended coordination dispatch algorithm based on the Stackelberg game with GA algorithm and PFM. Section 4 describes in detail the application of the PFM to the extended coordination dispatch algorithm. Section 5 presents the simulations using real data for the proposed extended coordination dispatch algorithm. Finally, Section 6 presents the concluding remarks.

The abbreviations and the key variables used in this paper are listed in Appendix A.

2. Mathematical representation

Figure 1 shows the structure of the microgrid (i.e. PVEVM) considered in this study, which is a combination of PV power generation and EV orderly charging. An ECC is employed as the coordinator that sells energy to the EV users and purchases energy from (or sells energy to) the wholesale grid market. In this study, we focus on the use of EV to help consume the PV output power locally. In this study, we focus on the use of EVs to locally consume the PV output power; hence, the energy storage system has not been considered.
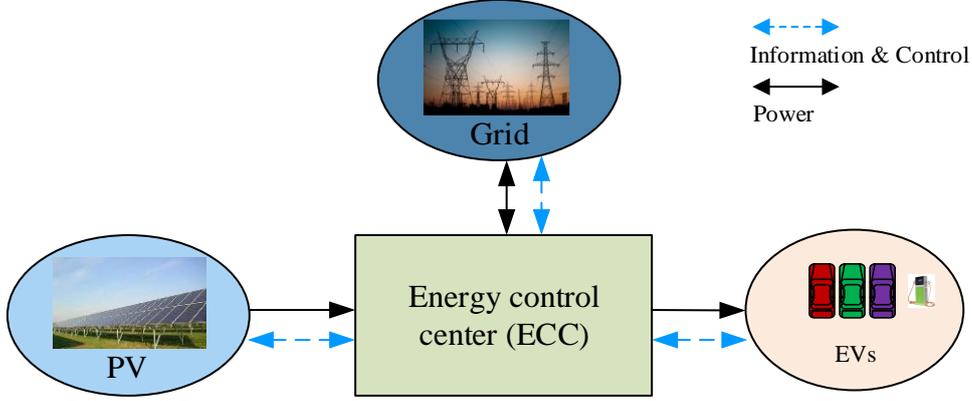
Fig. 1. Structure of the PVEVM

2.1. PVEVM energy trading model in the wholesale market

Owing to its capacity limitation, the PVEVM is taken as the price taker to participate in the day-ahead market (DAM) and real-time balancing market (RBM). Hence, the ECC of the PVEVM follows the following rules [28, 34]. First, before the end of trading in the energy market on day D, the ECC reports the energy trading information for the trading periods on day D+1 to the independent system operator (ISO) depending on the PV power generation and EV charging load curve, and considers the results of the ISO as the DAM energy curve. In the next RBM day, the ECC will determine whether it is necessary to purchase and sell electricity to the grid to balance the power deviation according to the PV real-time output and EV charging. After the end of the dispatch period, the ISO will impose additional penalties for PV abandonment to improve the level of PV consumption.

Under the ECC trading process described above, the key issue that requires to be addressed (by the ECC) is how to setting the retail electricity price for the next day to maximise profit. The optimisation problem for the PVEVM can be formulated as follows:

$$\max G = \max \sum_{t}\sum_{n} c_t u_{nt} + \sum_{t}(\pi_t^- E_t^- - \pi_t^d E_t - \pi_t^+ E_t^+), \ t \in \{1,2,\cdots,T\}, \ n \in \{1,2,\cdots,N\} \quad (1)$$

$$\text{s.t.} \quad c_t^1 \le c_t \le c_t^u, \pi_t^- \le \pi_t^d \le \pi_t^+, \ \forall t \quad (2)$$

$$\sum_{t=1}^{T} c_t / T = c_{av} \quad (3)$$

$$u_{nt} \ge 0, \ E_t \ge 0, \ 0 \le E_t^+ \le M, \ 0 \le E_t^- \le M, \ \forall t \quad (4)$$

$$\begin{cases} E_t^+ = \sum_i^N u_{nt} - P_t^{PV}, \; \sum_i^N u_{nt} \ge P_t^{PV} \\ E_t^+ = 0, \; \sum_i^N u_{nt} < P_t^{PV} \end{cases} , \; \forall t \tag{5}$$

$$\begin{cases} E_t^- = P_t^{PV} - \sum_i^N u_{nt}, \; \sum_i^N u_{nt} \le P_t^{PV} \\ E_t^- = 0, \; \sum_i^N u_{nt} > P_t^{PV} \end{cases} , \; \forall t \tag{6}$$

where, $\{c_t, u_{nt}, E_t, E_t^-, E_t^+, \forall t\}$ are the decision variables: c_t is the broadcasted price c at time t; c_t^l and c_t^h are the boundary values of the retail electricity price; c_{av} is the daily average broadcasted price; u_{nt} is the charging energy of the nth EV at time t; E_t and π_t^d are the contract energy and electricity price in the DAM, respectively; E_t^+ and E_t^- are the energy purchased from and sold to the RBM, respectively; π_t^+ and π_t^- are the corresponding electricity prices; M is the maximum traded energy in the RBM which can be set to the sum of the maximum charging energy of all the EVs; T is the number of time intervals; N is the number of EVs; and P_t^{PV} is the output of the PV power generation system; Eqs. (2) and (3) are the constraints of the broadcasted price while Eqs. (4), (5) and (6) together constitute the power balance condition to maximise the local PV consumption.

In the objective function shown in Eq. (1), there are four items that maximise the PVEVM's profit: the first item represents the income from selling electricity to the EV user; the second item is the income from selling electricity in the RBM; the third item is the cost of purchasing electricity in the DAM; the fourth item is the cost of purchasing from the RBM. Usually, the electricity price in the DAM is lower than that in the RBM, i.e. $\pi_t^d < \pi_t^+$.

2.2. PV power generation

The probability density function [28] and empirical formula [1] are used to calculate PV power generation. However, the PV power generation is nonlinear and depends on meteorological conditions, such as environment temperature, sunshine intensity, and rainfall, which are random and uncontrollable. The probability density function and empirical formula cannot consider the randomness and uncertainty. Accordingly, in this study, a PFM is used to forecast the PV power generation on the next day and send it to the ECC. We also employ intelligent algorithms based on real historical data, which can characterise the uncertainty of PV power generation. Section 4 will describe the PFM in detail.

2.3. EV charging and cost function

As described in [35, 36], for each EV user i, where $i \in \{1, 2, 3, \cdots, N\}$, at any time t, where $t \in \{1, 2, 3, \cdots, T\}$, the charging energy is demoted by u_{nt}, and the battery state of charge (SOC) is described by the following dynamic function:

$$s_{n,t+1} = s_{nt} + \frac{1}{\Theta_n} u_{nt}, \tag{7}$$

where Θ_n is the EV battery capacity, and s_{nt} is the normalised SOC for the nth EV at time t. Eq. (7) satisfies the constrains, shown in Eq. (8):

$$u_{nt} \begin{cases} \geq 0, \ when \ t \in \mathrm{T}_n \\ = 0, \ \text{otherwise} \end{cases}, \ \text{with} \ \sum_{t \in T} u_{nt} \leq \Gamma_n \tag{8}$$

Here, $\mathrm{T}_n \subset T$ denotes the charging horizon of the nth EV, $\Gamma_n = \Theta_n (s_{nM} - s_{n0})$ is the maximum energy of the nth EV, and s_{n0} and s_{nM} represent the initial and maximum SOC values, respectively, with $0 \leq s_{n0} \leq s_{nM} \leq 1$.

The cost function of the nth EV is given by the following expression:

$$\phi_n = \sum_{t \in T} c_t u_{nt} + \omega d_n (u_n), \tag{9}$$

where ω is a weight factor for the significance of EV user's satisfaction over the period T and $d_n(u_n)$ is the dissatisfaction cost [37], such that : $d_n(u_n) = e^{\beta_n (1 - (u_n / r_n))} - 1$, where β_n is the priority factor of the nth EV; and r_n is the reference demand of the nth EV, such that : $r_n = (s_{nr} - s_{n0}) \Theta_n$, where s_{nr} is the reference SOC value.

Then, the optimisation problem for each EV user can be formulated as follow, shown in Eq. (10):

$$\min \ \phi_n = \min \ \sum_{t \in T} c_t u_{nt} + \omega d_n (u_n) \tag{10}$$

2.4. Energy trading strategy in the PVEVM

It can be seen that different from the traditional optimisation problem, the profit of the PVEVM depends on the charging strategies employed by EV users, which are not directly controlled by the ECC but depend on the retail electricity price. The retail electricity price c_t broadcasted by the ECC depends on the PV power generation and EV charging load on the next day. Each EV user adjusts its charging demand u_{nt} based on the price broadcasted from the ECC. Consider the ECC and EV users as strategic players that make decisions that optimise their individual objectives. Because the daily average retail electricity price must be fixed, if the ECC raises the price for a certain period of time, the price in other periods will be lower than the average. Therefore, EV users will choose to charge their EV during the low-price period, when the SOC is in an acceptable range.

Assuming that the EV users are rational and will choose their charging strategy once they obtain the ECC's electricity price, and based on the interaction between the ECC and EV users, we formulate this energy trading process as a Stackelberg game, wherein the ECC is considered to be at the leader level and the EV users are considered to be at the follower level. The architecture of the Stackelberg game between the ECC and EV users is shown in Fig. 2.
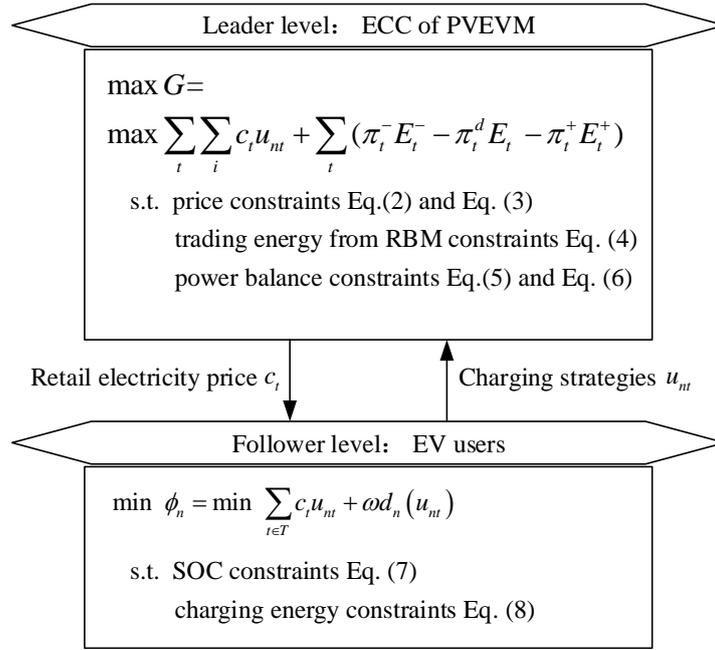
Fig. 2. Architecture of the Stackelberg game

3. Stackelberg game coordination dispatch

As described in the previous section, the decisions of the ECC and EV users are interdependent. EV users will rationally choose their strategy when the broadcasted price c is broadcasted by the ECC. To determine the real-time electricity price and the energy purchase strategy in the wholesale market, while accounting for the profit of the ECC and EV users, we establish a Stackelberg game, which considers the competition between the ECC and EV users.

3.1. Stackelberg game

There is a hierarchy among the players in Stackelberg games. Leaders are in the position to enforce their strategies on the followers. In other words, the competition in Stackelberg games is a leader-follower competition. In this competition, the followers find the best response once they observe the strategies of the leaders, of which the leaders are aware. Hence, the leaders can maximise their profit by anticipating the strategy response from the followers, which is the optimal strategy made by the followers for themselves after obtaining the decision of the leaders.

The following mathematical expression represents Stackelberg game is as follows [38, 39], shown in Eq. (11):

$$\begin{cases} \min_{x_i, y^*} F_i\left(x, y^*\right) \\ s.t.\ \mathrm{G}_i\left(x, y^*\right) \le 0 \\ H_i\left(x, y^*\right) = 0 \\ y^* \in S\left(x\right) \end{cases} \quad \forall i, \tag{11}$$

where x_i is the decision of the ith leader; $x = \left\{x^1,\ x^2, \cdots,\ x^m\right\}$, $y^* = \left\{y_1^*,\ y_2^*, \cdots,\ y_n^*\right\} \in S\left(x\right)$; then y_j is the decision of the jth leader, if and only if y_j^* is the Nash equilibrium for the follower:

$$\begin{cases} y_j^* = \arg \min_{y_j} \ f_j\left(x, y_j, y_{-j}^*\right) \\ \text{s.t. } g_j\left(x, y_j\right) \le 0 \qquad\qquad \forall j, \\ h_j\left(x, y_j\right) = 0 \end{cases} \tag{12}$$

where $y_{-j}^* = \left\{y_1^*, y_2^*, \cdots, y_{j-1}^*, y_{j+1}^* \cdots, y_n^*\right\}$. The above mathematical models above show that the game problem for the followers represents by Eq. (12) is actually the constraint conditions for the decision-making process of the leaders. In the Stackelberg game, the leaders make decisions x, and the followers make the optimal responses y^* to the decisions x. Finally, the leader makes the decisions x^*, which are most beneficial according to the decisions of the followers. $\left(x^*, y^*\right)$ is the Stackelberg equilibrium, which exists and is unique when the target functions and all constraints are convex [38, 40].

We introduce a one-leader, N-follower Stackelberg game, as shown in Fig. 2, to describe the electricity coordination dispatch between the ECC and EV users, where the ECC is the leader and the EV users are the followers. The electricity coordination dispatch system consists of the following four stages:

S1: The ECC broadcasts the broadcasted price c.

S2: Each EV user determines the best response $u^*(c)$ with respect to the broadcasted price c from the ECC.

S3: The ECC optimises the broadcasted price c^* considering the EV users' best response $u^*(c)$ from S2.

S4: Observing the ECC's best strategy, each EV user determines the optimal energy demand $u_n^*(c^*)$ for the broadcasted price c^* from S3.

Based on the above description, the electricity coordination dispatch optimisation problem can be formulated as follows:

Leader level (ECC):

$$c^* = \arg \max G\left(c; u^*\left(c\right)\right) \tag{13}$$

Follower level (EV users):

$$u_n^*\left(c\right) = \arg \min \phi_n\left(u_n; c\right) \tag{14}$$

The optimal strategies of the game take the form of the Stackelberg equilibrium [41, 42]. At the equilibrium, the leader's strategy c^* is a solution to the optimisation problem in Eq. (13) based on the best strategies $u_n^*(c)$ of the followers. Each follower's strategy is also an optimal solution to Eq. (14) when the follower receives the equilibrium strategy decision from the leader. Therefore, the optimal strategies $u_n^*\left(c^*\right)$ are the equilibrium for all the followers.

Stackelberg equilibrium definition: The strategy $\left(c^*, u^*\right)$ is a Stackelberg equilibrium *if it satisfies the following conditions:*

$$G\left(c^*; u^*\left(c^*\right)\right) \geq G\left(c; u^*\left(c\right)\right), \tag{15}$$

$$\phi_n\left(u_n^*; c^*\right) \geq \phi_n\left(u_n, \ u_{-n}^*; c^*\right), \quad \forall\, n \in N \tag{16}$$

where, $u_{-n}^* = \left[u_1^*, \ u_2^*, \cdots, \ u_{n-1}^*, \ u_{n+1}^*, \cdots, \ u_N^*\right]$.

Firstly, each follower, i.e. the EV user, determines the best strategy trajectory $u_n^*\left(c\right)$ by solving Eq. (15) with respect to a strategy of the broadcasted price c from the leader, i.e. the ECC. From Eq. (9), we have $\partial^2 \phi_n / \partial^2 u_n > 0$ thus, ϕ_n is a strictly convex function with respect to u_n [26, 40], and therefore there exist a unique optimal solution $u_n^*\left(c\right)$. Then, the ECC obtains its best strategy c^* using Eq. (16), depending on the best strategy trajectories from the EV users $u_n^*\left(c\right)$; c^* exists because $\partial^2 G / \partial^2 c > 0$. Subsequently, when the EV users receive the best strategy c^* from the ECC, they determine their best strategy $u_n^*\left(c^*\right)$. Thus, we have the Stackelberg equilibrium at $\left(c^*, u^*\right)$, which exists and is unique [38, 40]. A feasible solution for the proposed game in Eq. (15) and Eq. (16) is the Stackelberg equilibrium at which the ECC obtains its optimal price using the best responses of the EV users [27, 31].

3.2. Coordination dispatch algorithm

Fig. 3 shows a flowchart of the coordination dispatch algorithm based on the Stackelberg game, where K is the maximum number of the iterations.
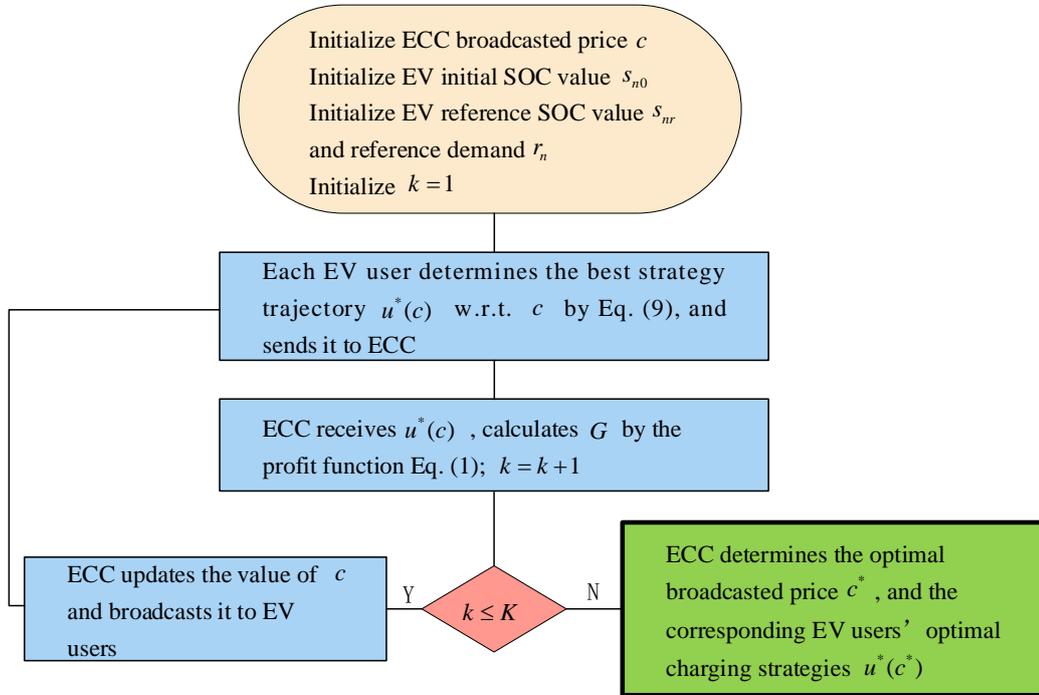

Fig. 3. Coordination dispatch algorithm based on the Stackelberg game

We use the GA to solve the optimisation problem in the proposed coordination dispatch. The GA which was proposed by Holland [43] is an efficient and effective global optimiser. It has been successfully applied in various fields, and is also applicable as a solution to the Stackelberg game problem in coordination dispatch [8, 28]. However, although this metaheuristic optimisation method already exhibits good performance in finding the Stackelberg equilibrium, there are still some areas that need improvement in its implementation [33]. Among these, optimisation of the initial population is the most relevant to this paper.

Therefore, to achieve the optimisation of the coordination dispatch algorithm proposed in this paper, the generation of the initial population for the broadcasted price c is critical. Herein, we propose a novel initial population generation method based on a PFM. The following steps are involved:

Q1: The PFM forecasts the PV power generation P_f^{PV} and EV charging load P_f^{EV} for the next day through intelligent algorithms and sends them to the ECC.

Q2: The ECC generates the initial population c_{init} of the broadcasted price c based on the forecasted data for PV power generation and EV charging load, shown in Eq. (17):

$$c_{init}^- \leq c_{init} \leq c_{init}^+ \tag{17}$$

Here,

$$c_{init,t}^- = \begin{cases} c_t^l, & \text{when } P_f^{PV} > P_f^{EV} \\ c_t^{ll}, & \text{when } P_f^{PV} \leq P_f^{EV} \end{cases}, \tag{18}$$

$$c_{init,t}^+ = \begin{cases} c_{av}, & \text{when } P_f^{PV} > P_f^{EV} \\ c_t^u, & \text{when } P_f^{PV} \leq P_f^{EV} \end{cases}, \tag{19}$$

$$c_t^{ll} = \begin{cases} c_t^l, & \text{when } c_{av} \leq c_t^l \\ c_{av}, & \text{when } c_{av} > c_t^l \end{cases}, \tag{20}$$

where c_{av} is the daily average of the retail electricity price.

The consumption of the PV power generation can be maximised by Eqs. (18)-(20); when P_f^{PV} is more than P_f^{EV}, the ECC lowers the broadcasted price to attract more EVs for charging, and when P_f^{PV} is lower than P_f^{EV}, the ECC raises the retail electricity price to reduce EV charging,–thereby reducing the risk of buying electricity from the RBM. The improved GA is named as the power forecasting-based GA.

Fig. 4 presents the flowchart of the extended coordination dispatch algorithm based on the Stackelberg game and power forecasting-based GA.
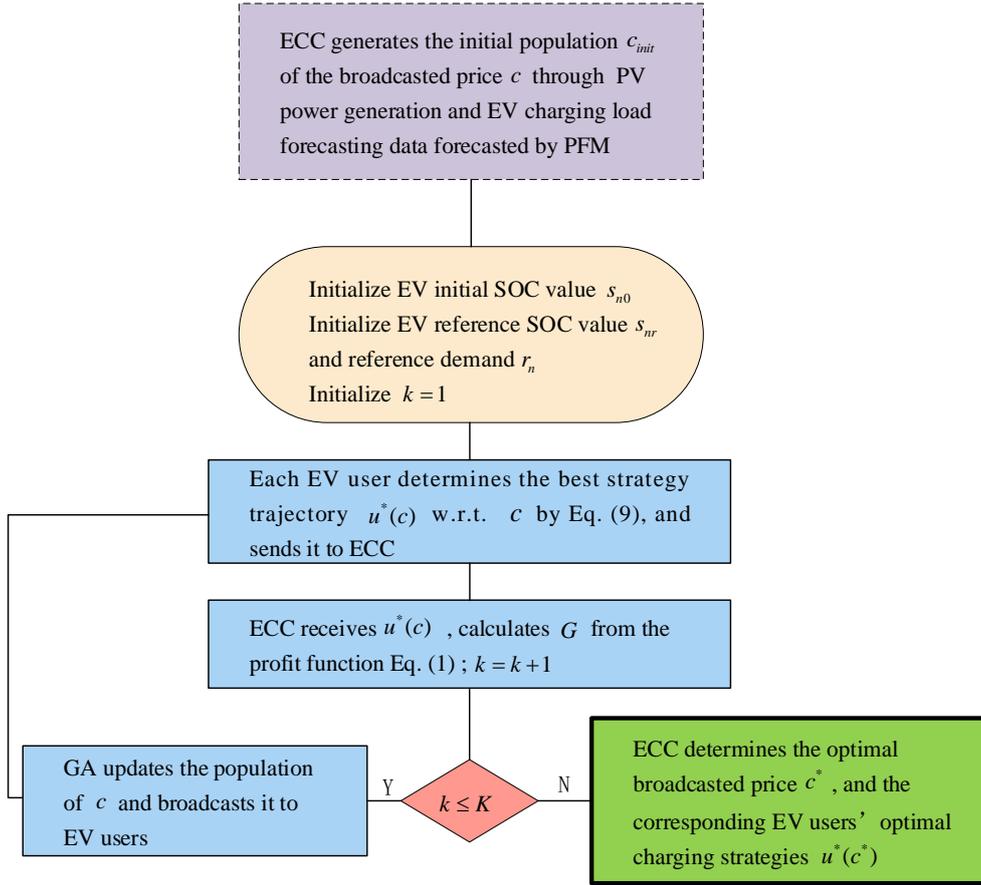
Fig. 4. Flowchart of the extended coordination dispatch algorithm

4. Power forecasting model (PFM)

As described in Section 3.2, the initial population of the GA will be generated according to the PV power generation and EV charging load data forecasted by the PFM. The intelligent algorithms in the PFM can consider the uncertainty by using the real historical data and a clustering algorithm-based generalized regression neural network (GRNN) for modelling, which is sufficiently capable of learning and generalization. The PFM includes two sub-models: PV power generation forecasting model and EV charging load forecasting model.

4.1. Correlation between power forecasting and meteorological condition

It is well known that the PV power generation fluctuates with meteorological conditions, particularly the environment temperature and sunshine intensity [44]. Many studies have been conducted on the PV power generation forecast based on meteorological conditions [45, 46].

The factors that influence the EV charging load can be categorised as internal and external. The internal factors include the EV battery size, charging mode, charging habits, and charging rate; the external factors include the time-of-use pricing (TOU) policy. The most critical internal factor is the charging habit, including the start of charging and one-day driving distance, which are difficult to measure. To characterise the charging habits, some studies have verified the correlation between charging habits and meteorological conditions, which is easy to measure by using data analysis and data mining techniques [47-50].

Due to the volatile and erratic nature of weather systems, the PV power generation and the EV charging load are always fluctuating, intermittent and random. The "uncertainty" is used to describe the inner stochastic traits of the PV power generation and the EV charging load in this paper in this study. The numerical weather prediction (NWP) data are used to build the PFM based on GRNN, which is well capable of learning and generalisation to learn the uncertainty information from the historical data.

The GRNN is a kind of radial basis function (RBF) neural network [51], with a typical structure, as shown in Fig. 5. It has three layers, namely the input, hidden, and output layers [52]: The input layer sends only the sample data (n dimensions) to the hidden layer. In the hidden layer, there is an activation function and the Gaussian function is most commonly utilised. The output layer uses a linear output (m dimensions).
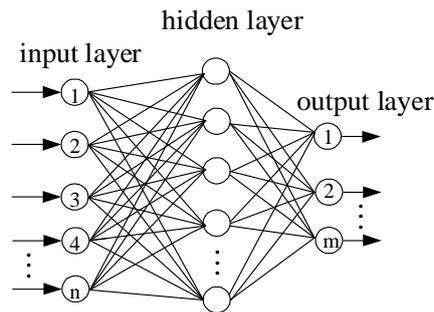
Fig. 5. Structure of the GRNN neural network

The GRNN exhibits a strong performance in non-linear fitting and regression problems [53], and is commonly used for various forecasting applications such as load, electricity price, and wind and PV power forecasting [51, 54]. Therefore, this case study uses GRNN as the prediction model. A schematic of the GRNN-based PFM using the NWP data as input and the power as output, is shown in Fig. 6.
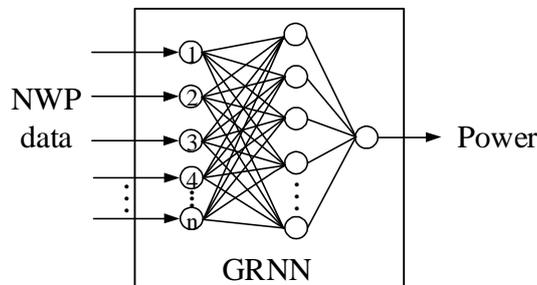
Fig. 6. Schematic of the GRNN-based PFM

4.2. PFM based on a clustering algorithm

During the training stage of the GRNN-based PFM shown in Fig. 6, high quality training samples can significantly improve the forecasting accuracy. As explained in Section 4.1, there is a high correlation between meteorological conditions and PV power generation and EV charging load. Hence, the days with similar PV power and EV charging load variation trends have similar meteorological conditions [55]. Therefore, the historical days with similar NWP information can be classified into one cluster, and choosing such historical days whose NWP information is similar to that of the forecasted day as training samples can improve the forecasting accuracy and reduce the computational complexity during the model simulation. The clustering algorithm is an effective tool for choosing high quality training samples [56].

13

We use the density peak optimized K-medoids (DPK-medoids) clustering algorithm [57] to cluster the historical data and select the training data for the GRNN. This algorithm is based on the K-medoids clustering algorithm, which is used to partition the dataset into clusters aiming to minimise the sum of the distances between the cluster samples and a central data point of the same cluster. It picks samples through centres (the medoids) and workings using the Manhattan Norm to express the distance among the data points [58]. The Manhattan Norm in this algorithm has been formulated as follows:

$$E=\sum_{i=1}^{k}\sum_{x\in C_i}\|x-c_i\|^2 ,\tag{21}$$

where c_i is the centre of the cluster C_i; and k is the number of clusters; besides, E also represents the distance within the cluster. The traditional K-medoids clustering algorithm is described as follows:

(1) Randomly select k samples of c_i as the initial centres;

(2) According to the principle of proximity, the remaining samples are allocated to the nearest cluster to form the initial partition. The distance between samples x and c_i is the following Euclidean distance: $d_i(x,c_i)=\sqrt{\sum_{a=1}^{p}(x_a-c_{ia})^2}, a=1,2,\cdots p$.

(3) Calculate the distance within the cluster E using Eq. (21), and the distance between the clusters B, as follows, shown in Eq. (22):

$$B = \sum_{i,j=1}^{k}\|c_i - c_j\|\tag{22}$$

(4) Calculate the criterion function Fit, shown in Eq. (23):

$$Fit = \frac{E}{B}\tag{23}$$

(5) Find a new centre for each cluster such that the sum of the distances from the other samples in the cluster to the new centre is minimised; replace the initial centre with the new centre, and calculate the criterion $Fit^{'}$.

(6) If $Fit^{'} < Fit$, return to the step (5); If $Fit^{'} \geq Fit$, end the clustering process.

(7) According to the distance between the samples and the cluster centre, cluster the sample dataset using the distance minimum principle.

However, a problem with the traditional K-medoids clustering algorithm is that the clustering result varies with the changes in the initial clustering centres; therefore, the DPK-medoids clustering algorithm was proposed as a solution [59]. The DPK-medoids consider the number of density peak points as the initial cluster centres, such that the initial cluster centre can be located in different clusters,

and the number of clusters is adaptively determined; this determination process involves the following three stages:

(1) Calculate the local density ρ_n and the distance σ_n of the sample x_n. The local density ρ_n is formulated as follow, shown in Eq. (24):

$$\rho_n = \frac{1}{\sum\limits_{j=1}^{N} d(x_n, x_j)}, \qquad (24)$$

where N is the number of the local nearest points, usually set to 6, 7, or 8, and the distance σ_n of the sample x_n is formulated as follow, shown in Eq. (25):

$$\delta_n = e^{\min\limits_{j:\rho_j > \rho_n} (d_{nj})} \qquad (25)$$

(2) Construct a decision graph for the distance relative to the density of x, the local density ρ is the horizontal axis, and σ is the vertical axis.

(3) Select the density peak points in the upper right corner of the decision graph, which is obviously far away from most samples in the dataset, as the initial cluster centres, and the number of the density peak points is the number of clusters.

A flowchart of the cluster analysis and GRNN-based PFM is shown in Fig. 7. There are two stages in the modelling: clustering with the DPK-medoids clustering algorithm, and then building the PFM through GRNNs. In the clustering stage, the NWP data of all historical days is used to identify the cluster to which the forecasted day belongs. Then, the days whose NWP information is similar to that of the forecasted day are chosen, and the NWP and power information of these days are used to train the prediction model. The power information here includes PV power generation and EV charging load data.

The datasets used for training and testing the GRNN-based PFM are described below.

Train Datasets: contains the NWP and power information of the days chosen by the DPK-medoids clustering algorithm.

Test Datasets: contains the NWP and power information of the forecasted day. The power here is used to evaluate the performance of the forecasting model.
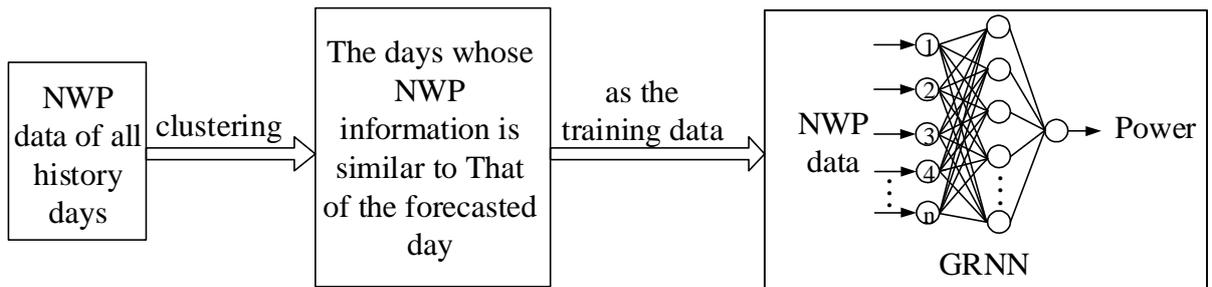
Fig. 7. Flowchart of the cluster analysis and GRNN-based PFM

4.3. PV power generation and EV charging load forecasting by the PFM

There are two PFMs: PFM for PV power generation (PVPFM) and PFM for EV charging load (EVPFM). They are all based on the PFM proposed above. The difference is the output of the GRNN: the GRNN in the PV power generation and EV charging load forecasting models outputs the PV power and EV charging power, respectively. The framework of the PFM is detailed in Fig. 8.
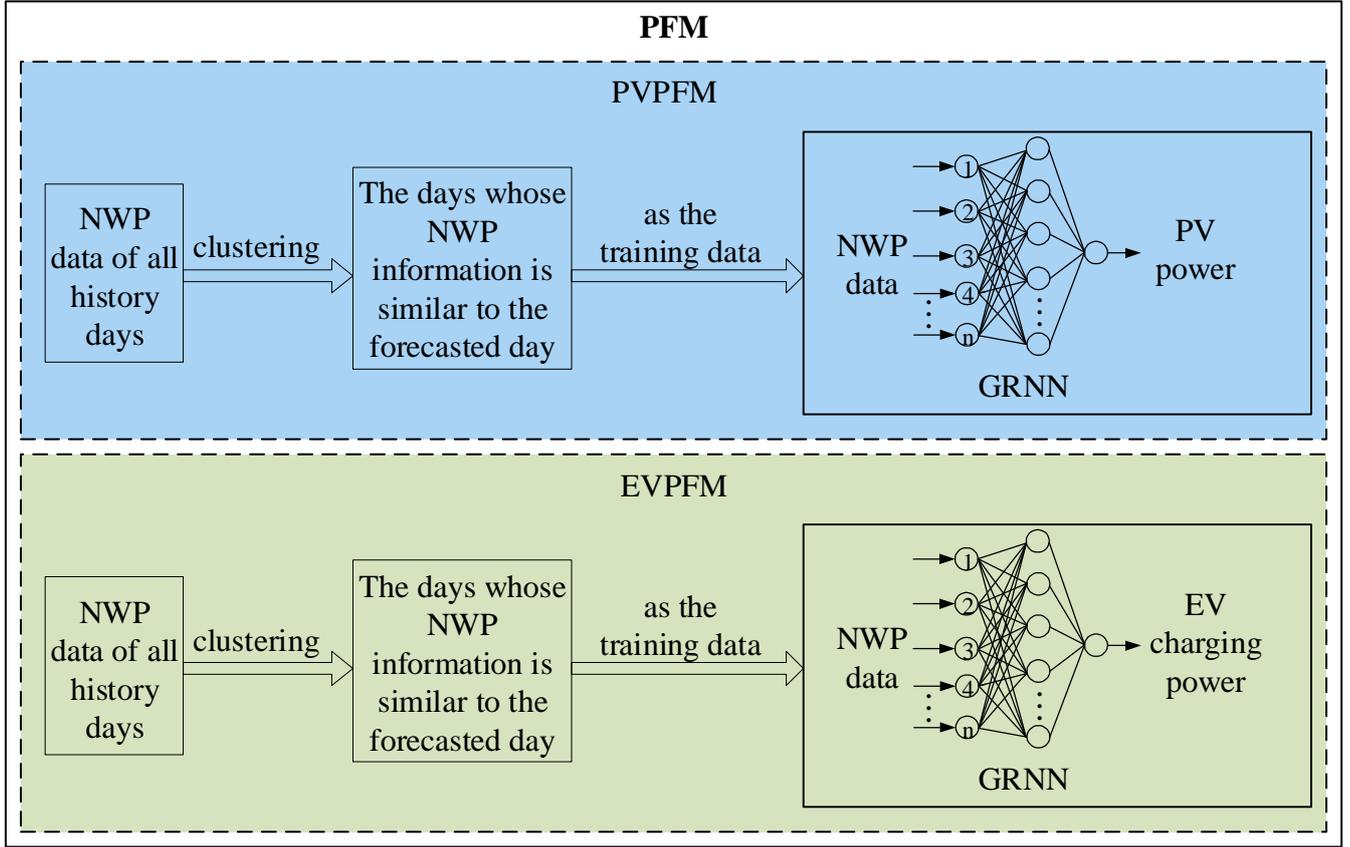
Fig. 8. Framework of the PFM

5. Case study

In this section, some simulations based on real data are used to analyse the extended coordination dispatch based on the Stackelberg game and GA presented in this paper. According to the description of the coordination dispatch, the case study is carried out in two parts: day-ahead PV power generation and EV charging load forecasting by PFM, coordinating EV orderly charging to maximise the profit of PVEVM and minimise the charging cost of EV users.

5.1. Day-ahead power forecasting by PFM

5.1.1. Database for day-ahead PV power forecasting model

Data from January 2017 to June 2018 from the Aifeisheng PV power station of 20MW capacity in Xinjiang Province, China, including the PV power generation from the PV power station and the NWP data, were used to build the day-ahead PV PFM through clustering, modelling, and forecasting.

After data cleaning and correlation analysis by Pearson correlation coefficient (PCC) and Rough Set (RS) [60], there are 332 days with NWP and PV power generation data. The NWP data includes

short-wave radiation (SR), long-wave radiation (LR), temperature (TM), 100 m wind speed (WS), cloud cover (CL), humidity (HU), momentum flux (MF), thermal flux (LF), 2 m humidity (HU_2),wind direction sine value (WD_S) and wind direction cosine value (WD_C), which show high correlation with PV power generation. The datasets are described in detail below.

Clustering dataset for PV:

This includes the daily NWP data, including the mean, maximum, and minimum values of the above-mentioned11 NWP factors , of the 332 days expressed as the following vector:

$$X^{PV} = \left[SR_{av}, SR_{max}, SR_{min}, LR_{av}, LR_{max}, LR_{min}, \cdots, D_{cmin} \right]_{332 \times 33}$$

Train dataset of GRNN for PV:

This includes the NWP and PV power information of for the days chosen from the clustering, including the 11 NWP factors and PV power. The temporal resolution is 15 min; besides, the data for the forecasted day has not been included in this dataset. The PV power generation P^{PV} is the output of the model. The train dataset can also be expressed as the following vector:

$$Train^{PV} = \left[SR, LR, TM, \cdots, HU_2, P^{PV} \right]_{(96*(n-1)) \times 12},$$

Where n is the number of days in the cluster to which the forecasted day belongs.

Test datasets of GRNN for PV:

This includes the NWP and PV power information of the forecasted day, with the same elements as the train dataset, expressed as the following vector:

$$Test^{PV} = \left[SR, LR, TM, \cdots, HU_2, P^{PV} \right]_{96 \times 12}$$

Here, the PV power is used to evaluate the performance of the forecasting model.

The timescale of forecasting is 1 day, and 96 forecasting steps are considered.

5.1.2. Database for day-ahead EV charging load forecasting model

Data from May to September 2012 of 321 EV charging stations in a London (UK) workplace parking, including the charging events and NWP data, were used to build the day-ahead EV PFM. After the same steps of data cleaning and correlation analysis as those used in the PV PFM, there are 147 days remaining for clustering. The NWP data includes global radiation (GR), temperature (TM), humidity (HU), wind direction sine value (WD_S) and wind direction cosine value (WD_C) which show a high correlation with PV power generation. Furthermore, we add weekday type and hour label into the data analysis, because there is an obvious relationship between the weekday type with EV user charging habits [61]. The following is a detailed description of the datasets:

Clustering dataset for EV:

This includes the daily statistic NWP data, including the mean, maximum, and minimum values of the above-mentioned five NWP factors. This dataset also includes the weekday type and can be expressed as the following vector:

$$X^{EV} = \left[GR_{av}, GR_{max}, GR_{min}, TM_{av}, TM_{max}, TM_{min}, \cdots, WD_{cmin} \right]_{147 \times 16}$$

Train dataset of GRNN for EV:

This is the same as that used for PV power generation forecasting. The EV charging load P^{EV} is the output of the model. The train dataset can be expressed as the following vector:

$$Train^{EV} = \left[GR, TM, \cdots, WD, P^{EV} \right]_{(96*(n-1)) \times 8}$$

The temporal resolution is 15 min, and the data of the forecasted day is not included in this dataset.

Test datasets of GRNN for EV: This includes the NWP and power information of the forecasted day, with the same elements as those in train dataset, and can be expressed as the following vector:

$$Train^{EV} = \left[GR, TM, \cdots, WD, P^{EV} \right]_{96 \times 8}$$

The EV charging power here is used to evaluate the performance of the forecasting model.

The timescale of forecasting is 1 day, and 96 forecasting steps are considered.

5.1.3. Verification of the PFM

A. DPK-medoids clustering

Following classification of the 332 historical days in the PVPFM and 147 historical days in the EVPFM based on the DPK-medoids clustering algorithm described in Section 4.3, respectively, the result shown in Table 1 and Fig. 9 were obtained. Figures 9 (a) and 9 (b) show the decision graphs in PVPFM and EVPFM. The number of clusters is four in PVPFM and three in EVPFM.

Table 1 Clustering results for PVPFM and EVPFM

PVPFM clusters				EVPFM clusters		
First	Second	Third	Fourth	First	Second	Third
4 days	213 days	26 days	48 days	21 days	26 days	100 days
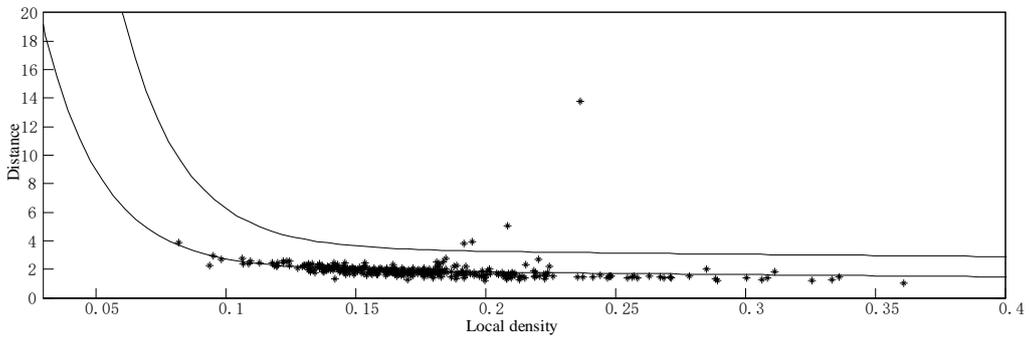
(a)
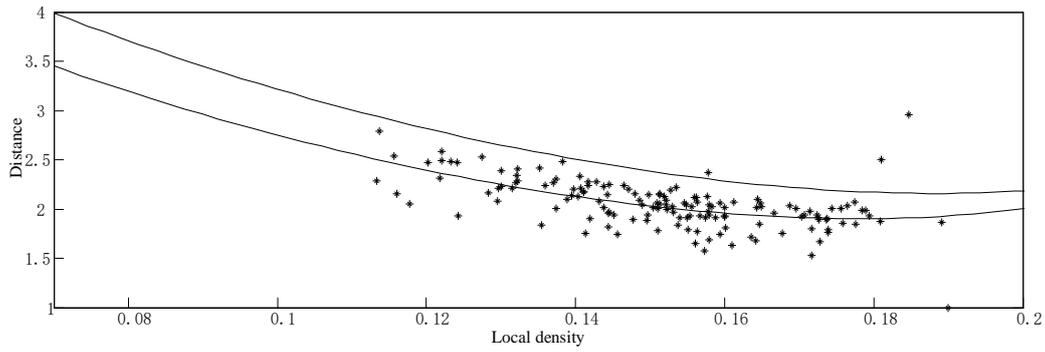
(b)

Fig. 9. The decision graph for the DPK-medoids clustering algorithm

B. PVPFM forecasting

To verify the performance of the PVPFM, the data in each cluster were divided into two datasets: The data from January 2017 to May 2018 were used as the train dataset, and that of June 2018 were used to as the test dataset. To further verify the effectiveness of the proposed model, the GRNN without clustering and the Markov chain (MCh) forecasting method, which has been explained in detail in Appendix B, were used to forecast the PV power generation using the same dataset. Table 2 shows the normalised root mean squared errors (NRMSEs) of the results forecasted for four days under different weather conditions. The forecasted results for 6 and 17 June 2018 are intuitively shown in Fig. 10 and Fig. 11. Furthermore, Table 2, Fig. 10, and Fig. 11 show that the proposed PVPFM can not only forecast with high accuracy on sunny days, but also exhibit high quality forecasting performance under the changeable weather conditions.

Table 2 Forecast errors on the different days

Forecasted day	Cluster to which the forecasted day belongs	Weather type	NRMSE (%)		
			Proposed PVPFM	MCH	GRNN
June 6, 2018	Second	Sunny	5.43	9.50	7.64
June 16, 2018	First	Cloudy	6.59	13.56	9.04
June 17, 2018	Second	Partly cloudy	7.41	8.31	11.96
June 21, 2018	Second	Shower	9.30	13.91	11.40
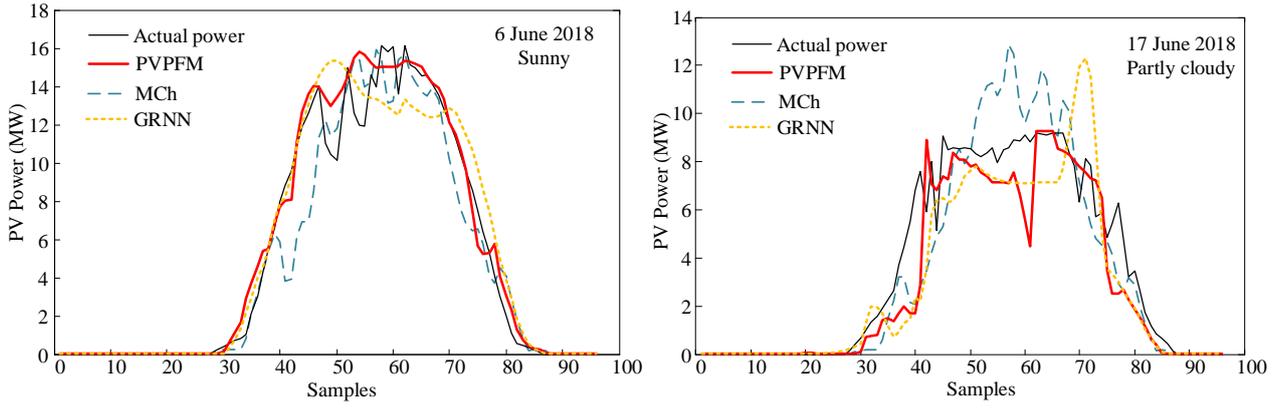
(a)   (b)

Fig. 10. PV power generation forecasted by different models
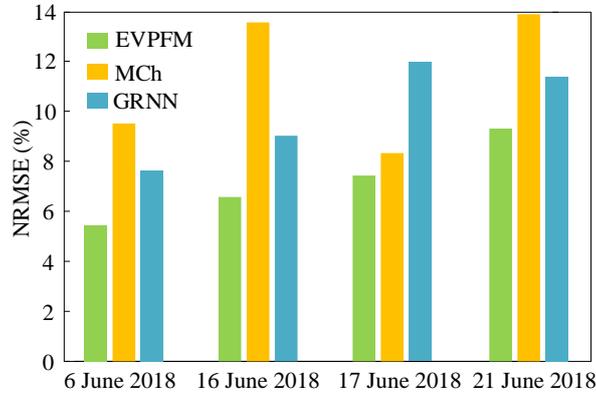
Fig. 11. Forecasted error of different models

C. EVPFM forecasting

The data from May to August 2012 were used as the train dataset, and that of September 2012 were used to as the test dataset. Besides, a GRNN forecasting model without clustering and a traditional forecasting method, namely the Monte Carlo (MC) forecasting model (which has been elaborated in detail in Appendix B) were used to further verify the effectiveness of the proposed model. Table 3 shows the NRMSEs of the forecast results for 25 to 30 September 2012, and Fig. 12 intuitively shows the forecast results for 25 and 27 September 2012. Furthermore, Table 3 and Fig. 12–13 show that the EVPFM can effectively characterise the uncertainty of EV charging load by using the clustering algorithm and neural network.

Table 3 Forecast errors on the different days

Forecasted day	Cluster to which the forecasted day belongs	NRMSE (%)		
		Proposed PVPFM	MC	GRNN
25 September 2012	Third	2.89	3.14	3.89
26 September 2012	Second	6.61	6.45	6.71
27 September 2012	First	2.91	5.54	3.12
28 September 2012	Third	5.68	7.05	7.07
29 September 2012	Third	5.47	5.89	5.95
30 September 2012	Third	4.43	5.55	4.87

(a)   (b)

Fig. 12. EV charging load forecasted by different models

Fig. 13. Forecasted error by different models for EV charging load

D. Evaluation of the PFM

The following deductions can be made from the Table 2−3 and Fig. 10−13:

1) The NRMSE histogram and the forecasting curve show that the forecasting performance of the proposed PFM is the best among the forecasting models used in this case study.
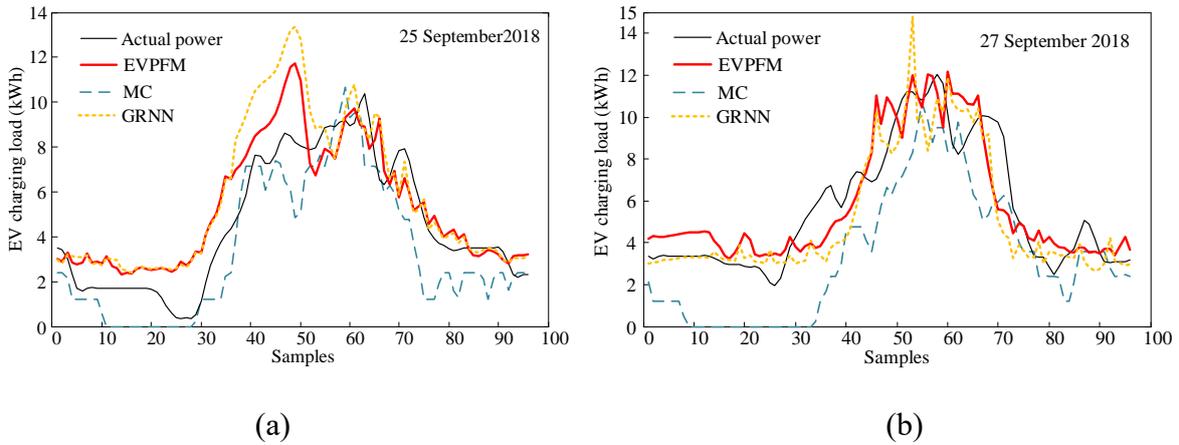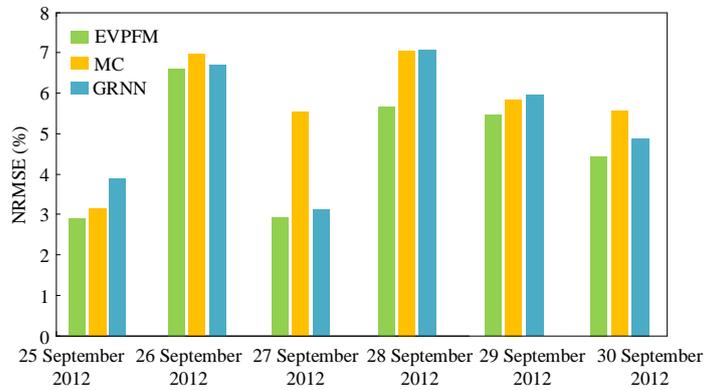
2) GRNN is well capable of learning and generalisation. However, the GRNN without the clustering model can predict only the trend, but not the volatility of the power; moreover, there are some points with significant errors in the forecasted power curves. This is because the training data used by this model comprises all historical samples. There is a large amount of information low related to the forecasted day, which reduces the forecasting accuracy.

3) Although the MCH forecasting model exhibits good forecasting performance, such as that on 17 June 2018, there are significant forecasting errors on other days, e.g. on 16 June 2018. This is because while the MCH method is suitable to describe a problem with large stochastic volatility, its forecast is only based on the historical power data and the change in the current state. Therefore, this model does not have the ability to learn and generalise.

4) The MC forecasting model exhibits a forecasting performance similar to that of the MCH forecasting model: while the NRMSE for 25 September 2012 is 3.14, it is 7.05 for 28 September 2012. This is because the MC method only simulates the EV charging event according to the empirical probability distribution of the charging parameters, which does not allow the characterisation of the uncertainty of the EV charging load.

In summary, the proposed PFM has a good power forecasting ability for the following reasons:

1) It uses GRNN as the training model, which can learn the information from the historical NWP data and power data to characterise the uncertainty of the PV power generation and EV charging load.
2) It chooses the historical days with NWP information, which are similar to the forecasted day, as the model training samples using the DPK clustering algorithm.

Thus, it improves the forecasting accuracy and the learning ability of the forecasting model, as it can effectively characterise the uncertainty of the PV power generation and the EV charging load.

5.2. Coordination dispatch between PVEVM and EV users

To demonstrate the performance of the proposed coordination dispatch algorithm, especially under changeable weather conditions, the data of 17 June 2018 were used. As described in Fig. 2 and Fig.4, we specified Algorithm 1 for the EV user and Algorithm 2 for the PVEVM to determine the Stackelberg equilibrium, as it can maximise the profit of the PVEVM and minimise the charging cost of the EV users. The 400 kW capacity of the Aifeisheng PV power station was studied to match the charging demand of the EVs, of which the initial SOC s_{n0} was randomly generated between 0.2 and 0.5. The EV parameters were assumed to be the same, as shown in Algorithm 1. The simulation ran from 8:30 to 21:30 and the length of each time interval was 30 min. The electricity prices in the Xinjiang Province are described in Table 4.

Algorithm 1: Solution to minimise charging cost for the EV users

---

GA method for the charging cost for EV users

1: **Input:** The broadcast broadcasted price c by ECC.

2: **Initial:** The initial population of EV charging energy $u_{nt,init}$;

The number of iterations $gen = 100$;

$T = 14$, $\Theta_n = 30 \, kWh$, $s_{nM} = 1$, $s_{nr} = 0.5$, $\omega = 0.1$, $\beta_n = 2$;

The maximum charging power $P_{\max} = 5kWh$, s_{n0} is randomly generated between 0.2 and 0.5.

3: Repeat

$k = 1$;

4: Calculate ϕ_n from the charging cost function;

5: Perform selection, crossover, and mutation operation;

6: Generate offspring population for EV charging power u_{nt}^k ;

7: $k = k + 1$;

8: Execute Step 4 until $k = gen$;

9: **Output:** The best strategy trajectory $u^*(c)$.

Algorithm 2: Solution method to maximise the PVEVM profit using the power forecasting-based GA

GA method for PVEVM profit

1: **Initial:** Generates the initial population c_{init} of the broadcasted price c through the PV power generation and EV charging load forecast data by Eqs. (18)-(20);

The number of iterations $gen = 100$;

$T = 14$;

$c_{av} = 0.7$, and other electricity prices shown in Table 4.

3: Repeat

$k = 1$;

4: Calculate ϕ_n using Algorithm 1 for each individual in the population;

5: Calculate PVEVM profit G using Eq. (1);

5: Perform selection, crossover, and mutation operation;

6: Generate offspring population for the broadcasted price c^k ;

7:	$k = k + 1$;
8:	Execute step 4 until $k = gen$;

9: **Output:** The best strategy c^*.

Table 4 Electricity prices in Xinjiang Province between 8:30 and 21:30

Time	π_t^d	π_t^+	π_t^-	c_t^u	c_t^1
8:30	0.48	0.77	0.19	0.77	0.38
9:00	0.48	0.77	0.19	0.77	0.38
10:30	0.76	1.22	0.30	1.22	0.61
11:30	0.76	1.22	0.30	1.22	0.61
12:30	0.76	1.22	0.30	1.22	0.61
13:30	0.48	0.77	0.19	0.77	0.38
14:30	0.48	0.77	0.19	0.77	0.38
15:30	0.48	0.77	0.19	0.77	0.38
16:30	0.48	0.77	0.19	0.77	0.38
17:30	0.48	0.77	0.19	0.77	0.38
18:30	0.48	0.77	0.19	0.77	0.38
19:30	0.76	1.22	0.30	1.22	0.61
20:30	0.76	1.22	0.30	1.22	0.61
21:30	0.76	1.22	0.30	1.22	0.61

A. Forecasted data for PV power generation and EV charging load

The forecasted data for PV power generation and EV charging load from the PFM for 17 June 2018 are shown in Fig. 14.
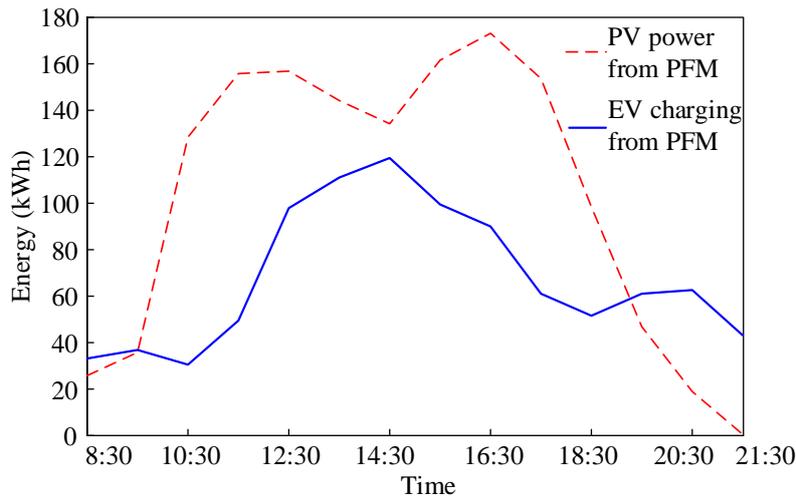

Fig. 14. Forecasted data for PV power generation and EV charging load-from the PFM

We observe that PV power generation is significantly higher than the EV charging load forecasted by the PFM using historical data, between 9:30 and 19:30. Therefore, to avoid PV consumption and

additional penalties, the ECC needs to guide more EV users for charging during this period by determining the effective broadcasted price strategy. This broadcasted price could also maximise the PV consumption and ensure profit for the PVEVM as well as the EV users. The best strategies for the broadcasted price and EV charging energy are represented by the Stackelberg equilibrium $\left(c^*, u^*\right)$ in this proposed coordination dispatch, which is achieved by using Algorithm 1 and Algorithm 2. The number of EVs participating in the coordination dispatch was set to 80 for this case study.

B. Initial population of the broadcasted price in Algorithm 2

As described in Section 3.2, the ECC generates the initial population c_{init} for the broadcasted price c through the PV power generation and EV charging load forecasted data using Eqs. (18)-(20) to maximised the local consumption of PV power generation. The boundary values for the initial population c_{init} on 17 June 2018 based on the forecasted data shown in Fig. 14 are shown in Table 5 and Fig. 15. The normal boundary values for the retail electricity price c_t^l and c_t^u from the government were used here for comparison, and named as Normal case. These two initial population generation methods were used in the Proposed case and the Normal case, respectively, and the comparison results were analysed in this study.

Table 5 Boundary values for the initial population

Time	c_{init}^+	c_{init}^-	c_t^u	c_t^l
8:30	0.77	0.70	0.77	0.38
9:00	0.77	0.70	0.77	0.38
10:30	0.70	0.61	1.22	0.61
11:30	0.70	0.61	1.22	0.61
12:30	0.70	0.61	1.22	0.61
13:30	0.70	0.38	0.77	0.38
14:30	0.70	0.38	0.77	0.38
15:30	0.70	0.38	0.77	0.38
16:30	0.70	0.38	0.77	0.38
17:30	0.70	0.38	0.77	0.38
18:30	0.70	0.38	0.77	0.38
19:30	1.22	0.70	1.22	0.61
20:30	1.22	0.70	1.22	0.61
21:30	1.22	0.70	1.22	0.61
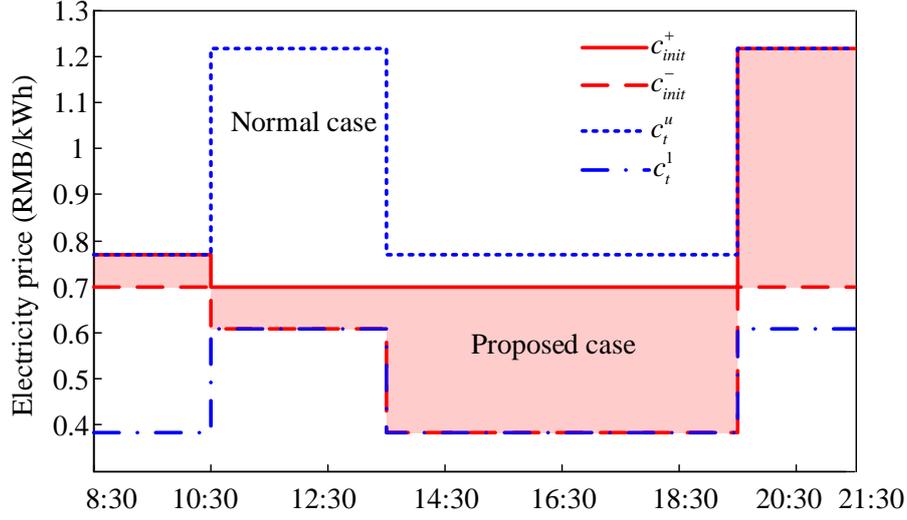
Fig. 15. Boundary values of the initial population used in Proposed case and Normal case

C. Processes in the coordination dispatch

As observed from Eq. (1), there are two processes in the coordination dispatch:

The first process concerns the DAM, i.e. the term $\sum_t \pi_t^d E_t$, wherein the ECC determines the contract energy E_t for the next day based on the forecasted data for PV power generation and EV charging load. Here, the value of E_t is calculated by using the day-ahead power forecasting made by PFM, as discussed in Section 5.1; the detailed data are presented in Table 6.

Table 6 Forecasted data and contract energy in the DAM

Time	P_f^{PV} (kWh)	P_f^{EV} (kWh)	E_t (kWh)
8:30	32.95	25.58	7.37
9:00	36.53	35.54	0.99
10:30	30.28	127.99	0
11:30	49.18	155.56	0
12:30	97.66	156.67	0
13:30	111.04	143.98	0
14:30	119.21	134.17	0
15:30	99.30	161.42	0
16:30	89.53	172.68	0
17:30	60.63	153.42	0
18:30	51.42	98.40	0
19:30	60.99	46.82	14.17
20:30	62.19	18.56	43.36
21:30	42.84	0.44	42.40

The second process concerns the RBM, i.e. the term $\sum_t \sum_n c_t u_{nt} + \sum_t (\pi_t^- E_t^- - \pi_t^+ E_t^+)$. The extended coordination dispatch algorithm proposed in this paper is used to simulate this RBM process based on the initial population c_{init}, Algorithm 1, and Algorithm 2, followed by the best broadcasted price c^* and the optimal charging strategies for each EV user, as shown in Fig. 16 and Fig. 17; these can be obtained according to the game between the ECC and EV users.

As shown in Fig. 14, the forecasted EV charging energy before 9:30 and after 19:30 is higher than the forecasted PV power generation; therefore, the broadcasted price c^* in the Proposed case is closer to the peak price boundary. On the other hand, between 9:30 and19:30, the PV power generation significantly exceeds EV charging load. Therefore, to sell more PV energy to EV users, the broadcasted price c^* in Proposed case varies between the valley price and the average price stipulated by the grid. Besides, it can be seen that the price purchased from the RBM π_t^+ is at the peak price between 19:30 and21:30, therefore c^* close to the peak boundary not only reduce EV charging load but also improve the profit of the PVEVM. For a more intuitive demonstration, the broadcasted prices in the two cases are listed in Table 7. The actual PV power generation on 17 June 2018 and the total EV charging energy of 80 EVs are shown in Fig. 14. Compared with the Normal case, the proposed coordination dispatch exhibits a better PV power consumption. Table 8 shows the PV abandonment rate in the two different coordination dispatch cases and the scenario without the coordination dispatch. We observe that the extended coordination dispatch algorithm can improve the local PV consumption.
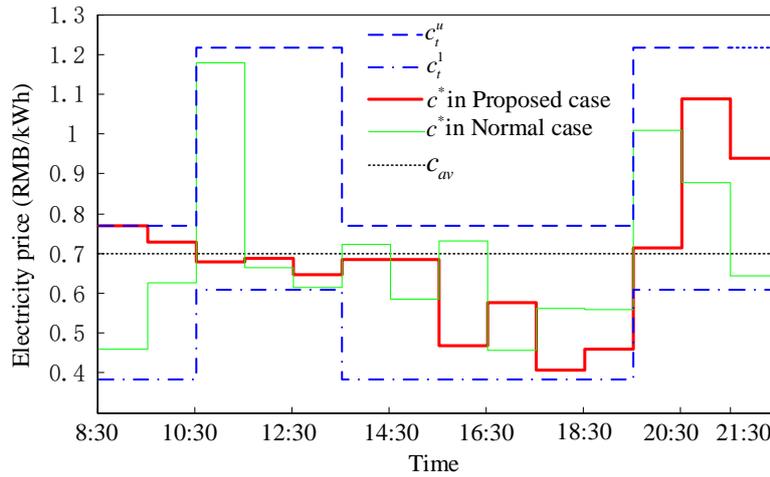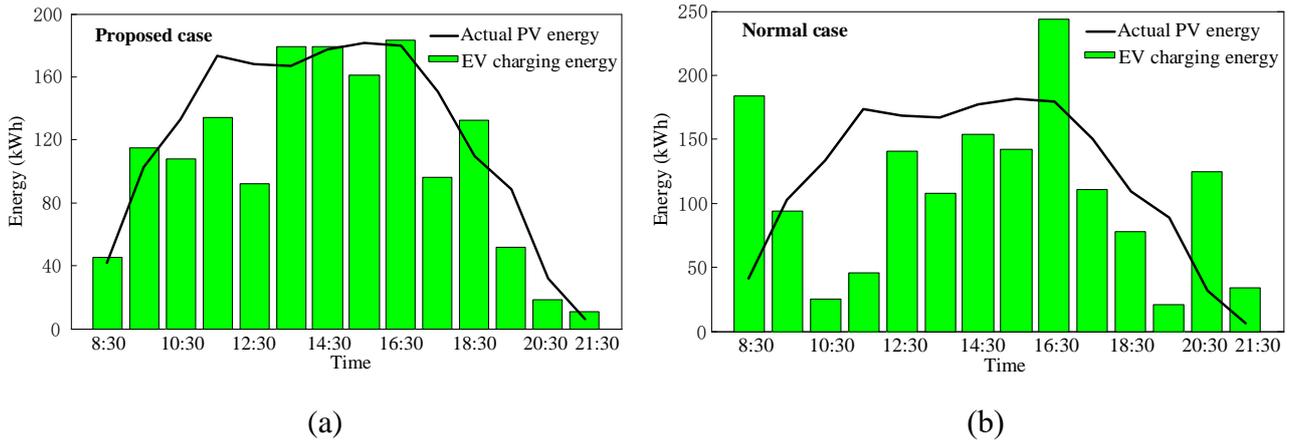

Fig. 16. Broadcasted price c^*

Fig. 17. Total EV charging energy of 80 EVs

Table 7 Best broadcasted price in the two cases

Time	c^* in Proposed case	c^* in Normal case
8:30	0.77	0.46
9:00	0.73	0.63
10:30	0.68	1.18
11:30	0.69	0.66
12:30	0.65	0.61
13:30	0.68	0.72
14:30	0.69	0.59
15:30	0.47	0.73
16:30	0.58	0.46
17:30	0.41	0.56
18:30	0.46	0.56
19:30	0.71	1.01
20:30	1.09	0.88
21:30	0.94	0.64

Table 8 PV abandonment rate in different cases

Without coordination dispatch	Proposed case	Normal case
0.49	0.15	0.31

D. PVEVM profit and EV charging cost

The profit of PVEVM and the charging cost of 80 EV users were calculated, and Table 9 presents the values in the two cases, i.e. the Proposed case and Normal case. The charging costs of the EV users are approximate, and we observe that the profit of the PVEVM in the Proposed case is considerably higher than that in the Normal case. This is because before 9:30 and after 20:30, the PVEVM in the Normal case needs to purchase electricity at a high price from the RBM to meet the EV charging

28

demand. Besides, it is worth mentioning that the coordination dispatch based on Stackelberg game is effective in terms of describing the competition between the PVEVM and EV users, because the profit of PVEVM is 814.22 and the average of the EV charging price is 0.70, when there is no coordination dispatch.

Table 9 Profit of PVEVM and the charging cost of 80 EV users

Proposed case			Normal case		
PVEVM profit (RMB)	Charging cost of 80 EV users (RMB)	Average of the EV charging price (RMB)	PVEVM profit (RMB)	Charging cost of 80 EV users (RMB)	Average of the EV charging price (RMB)
2605.76	1026.65	0.68	2412.72	1039.24	0.69

To further verify the effectiveness of the proposed model, the performance of the extended coordination dispatch on the other three days mentioned in Section 5.1.2 under different weather types is presented in Table 10.

Table 10 Profit of PVEVM and charging cost of 80 EV users

Date	Proposed case			Normal case		
	PVEVM profit (RMB)	Charging cost of 80 EV users (RMB)	PV abandonment rate	PVEVM profit (RMB)	Charging cost of 80 EV users (RMB)	PV abandonment rate
June 6, 2018	4480.04	1026.65	0.42	4418.18	1065.42	0.54
June 16, 2018	1369.27	1047.53	0.10	1344.8	1073.46	0.22
June 21, 2018	728.98	1051.04	0.32	642.42	1088.56	0.42

E. Analysis of the efficiency and stability

The objective of Algorithm 2 is to optimise the profit of the PVEVM—the leader of game, which continues to grow in the iterative process. On the other hand, the objective of Algorithm 1 is to minimise the costs for the EV users—the followers of the game, who respond to the prices generated from the ECC of PVEVM. Their charging costs are sensitive to the broadcasted price strategy and decrease as the number of interactions increases until the profit (of PVEVM) and the costs (of EV users) converge. The PVEVM profit and the costs of the EV users reach the equilibrium point through the Stackelberg game, which is the convergence point in the coordination dispatch algorithm. The optimisation iterative process of PVEVM profit is shown in Fig. 18. We observe that the curve based on the extended coordination dispatch algorithm proposed in this paper tends to converge after about 19 iterations, as shown in Fig. 18 (a), while in the Normal case, the number of such iterations is 42, as shown in Fig. 18 (b). Thus, we observe that the extended coordination dispatch algorithm requires fewer iterations to achieve the convergence. Therefore, the proposed power forecasting-based GA not only improves the profit of the PVEVM, but also quickens the convergence.
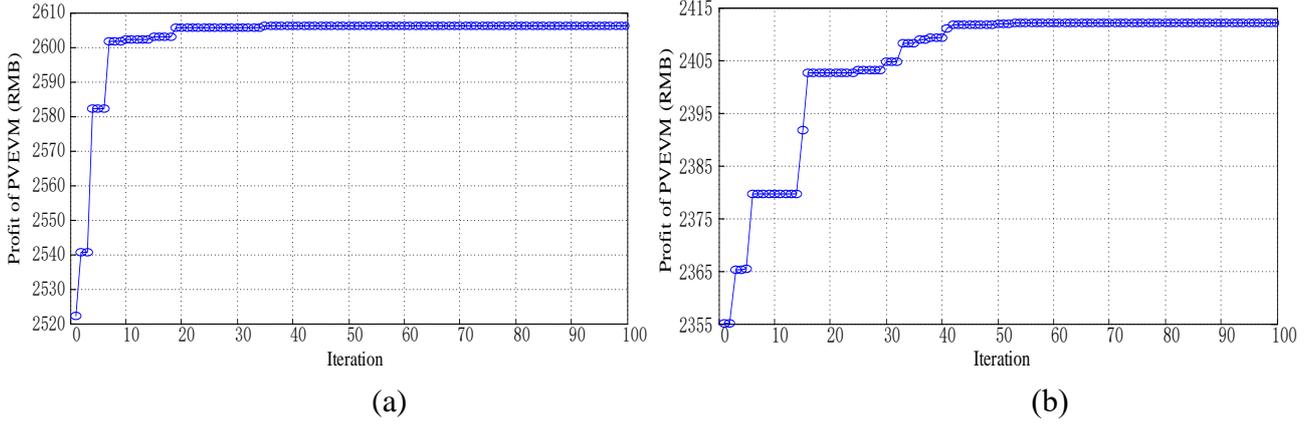
Fig. 18. Iterative process in the two different cases

5.3. Evaluation of the extended coordination dispatch

In summary, the comparison and statistical test results reveal the following:

(1) Compared with the traditional forecasting model, the PFM which is based on a clustering algorithm and GRNN using real history data can characterise the uncertainty of PV power generation and EV charging load. The simulation of the energy coordination dispatch based on PV power generation and EV charging is closer to the actual scenario.

(2) The Stackelberg game established in this paper can describe the competitive interaction between the PVEVM and EV users. In the case study both the Proposed case and Normal case are better than the scenario without coordination dispatch, in terms of the local consumption of PV, the profit of PVEVM and the cost of EV users. Moreover, compared with the Normal case, the Proposed case using the extended coordination dispatch algorithm based on power forecasting-based GA exhibits the better performance.

(3) Compared with the Normal case with price boundary imposed by the government, the initial population generated by the power forecasting-based generation method using the new boundary values proposed in this study can improve the performance of GA to achieve the Stackelberg equilibrium. This method reduces the boundary of the initial population, and generates a more reasonable initial population, which in turn improves the quality of the initial population and the efficiency of the subsequent operations of the GA (e.g. selection, crossover, and mutation).

6. Conclusions

We proposed an extended coordination dispatch algorithm based on the Stackelberg game, which considers the uncertainty of PV power generation and EV charging load through a PFM based on DPK-medoids clustering algorithm and GRNN. We established the optimisation problem for PVEVM considering EV user charging payments, the trading cost in the DAM and RBM, and the PV local consumption. An EV charging cost function considering the dissatisfaction cost was formulated. Based on the interplay between the PVEVM and EV users during the energy trading process, a one-leader multiple-follower Stackelberg game with improved GA was established to determine the real-time broadcasted price and the energy purchase strategy while considering the profit of the PVEVM and the EV users. At the Stackelberg equilibrium, the PVEVM obtains the maximum profit and guides the

EV users orderly charging through the broadcasted price. Thus, the EV users pay the minimum charging cost responding to the broadcasted price. The improved GA with a specific initial population is applied to solve the optimisation problem, which has been named as the power forecasting-based GA. The specific initial population of the improved GA, which is generated by the PV power generation and EV charging load day-ahead forecasted data using the PFM, could improve the performance of the GA to achieve the Stackelberg equilibrium. Finally, real data from a PV power station in China and 321 EV charging stations in the UK were used to verify the performance of the proposed coordination dispatch algorithm.

In this study, we only solved the optimisation problem between one PVEVM and EV users considering the broadcasted price. In our future work, we plan to structure a coordination dispatch between multiple PVEVMs in different areas with EV users considering their travel habits. Furthermore, it would be useful to consider the charging waiting time in the coordination dispatch. Hence, as a continuation, we will conduct more research on the coordination dispatch of PV power generation and EV charging. Besides, as the power forecasting-based initial population generation method for the GA proposed in this paper is effective in terms of improving the optimisation performance of the GA, it can also be considered for improving other metaheuristic optimisation algorithms in future research.

Conflicts of interest

The authors declare that there are no conflicts of interest regarding the publication of this paper.

Acknowledgement

Appendix A

Table 11 Abbreviations

EV	Electric vehicle
RESs	Renewable energy sources
PVEVM	PV power generation microgrid with plug-in EVs
ECC	Energy control centre
GA	Genetic algorithm
PSO	Particle swarm optimization
GRNN	Generalized regression neural network
DPK-medoids	Density peak optimized K-medoids
DE	Differential evolution
MCH	Markov chain
MC	Monte Carlo
PFM	Power forecasting model
PVPFM	PFM for PV power generation
EVPFM	PFM for EV charging load
DAM	Day-ahead market
RBM	Real-time balancing market
ISO	Independent system operator
SOC	Battery state of charge

Table 12 Variables and parameters

t	Time interval, $t \in \{1, 2, \cdots, T\}$
n	Index of the EV, $n \in \{1, 2, \cdots, N\}$
G	PVEVM's profit
c	Broadcasted price from the ECC
c_t	Broadcasted price c at time t
c_{init}	Initial population of the broadcasted price c in the GA
c^k	The kth offspring population of the broadcasted price c in the GA
u_n	Charging energy of nth EV
u_{nt}	Charging energy of nth EV u_n at time t
$u_{nt,init}$	Initial population of the EV charging energy u_{nt} in the GA
u_{nt}^k	The kth offspring population of the EV charging energy u_{nt} in the GA
E_t^-	Energy sold to the RBM
E_t^+	Energy purchased from the RBM
c_t^1, c_t^u	Boundary values of the broadcasted price c_t
c_{av}	Daily average broadcasted price
P^{PV}	Output of the PV power generation system
P_f^{PV}	Forecasted value of the PV power generation by the PFM
P^{EV}	EV charging load
P_f^{EV}	Forecasted value of the EV charging load by the PFM
M	Maximum traded energy in the RBM
ϕ_n	Cost function of the nth EV
ω	Weight factor of the significance of the EV user satisfaction over the period T
$d_n(u_n)$	Dissatisfaction cost of the nth EV
β_n	Priority factor of the nth EV
r_n	Reference demand of the nth EV
s_{nt}	Normalised SOC for the nth EV at time t
Θ_n	Battery capacity of the nth EV
P_{max}	Maximum charging power
T_n	Charging horizon of the nth EV, $T_n \subset T$
Γ_n	Maximum energy of the nth EV

s_{n0}	Initial SOC value
s_{nM}	Maximum SOC value
s_{nr}	Reference SOC value
$\left[SR_{av}, SR_{max}, SR_{min}, LR_{av}, LR_{max}, LR_{min}, \cdots, D_{cmin}\right]$	Mean, maximum, and minimum values of the 11 NWP factors for PV power generation
$\left[GR_{av}, GR_{max}, GR_{min}, TM_{av}, TM_{max}, TM_{min}, \cdots, WD_{cmin}\right]$	Mean, maximum, and minimum values of the five NWP factors for EV charging load

Appendix B

B.1 Markov chain (MCh) forecasting model for PV power generation

The Markov chain (MCh) model can forecast a future trend which is based on certain variables and changes in the existing state. It is suitable for describing a problem with large stochastic volatility [62, 63]. The MCH forecasting method is a probabilistic forecasting method which studies the transition probability between the states to determine the overall variation trend and predict the future state of the system.

We assume that the state space of a random process $\{X_m\}$ is $H = \{h_0, h_1, \cdots, h_N\}$, the current state is h_i, and the next state is h_j; then, the transition probability is expressed as follows:

$$P\{X_{t+1} = h_j \mid X_t = h_i\} = P_{ij} = \frac{F_{ij}}{F_i}, \tag{26}$$

where P_{ij} is independent of t, F_{ij} is the data sample which transfer one-step from the state h_i to the state h_j, and F_i is the data sample in state h_i. The matrix P is defined as follows:

$$P = [P_{ij}] = \begin{bmatrix} P_{11} & P_{12} & \cdots & P_{1N} \\ P_{21} & P_{22} & \cdots & P_{2N} \\ \vdots & \vdots & \vdots & \vdots \\ P_{N1} & P_{N2} & \cdots & P_{NN} \end{bmatrix} \tag{27}$$

It is known as the one-step transition probability matrix for the chain matrix and satisfies the following two properties: $P_{ij} \geq 0$, $\sum_j P_{ij} = 1$. The state transition probability matrix has the ability to track randomly fluctuating variables with the "non-aftereffect property", i.e. P_{ij} only depends on the state $X_t = h_i$ at time t, and not on the state before time t.

The solution of the MCH forecasting model for PV power generation involves the following steps:

(1) Divide the historical PV power generation data into N state intervals, i.e. the state space $H = \{h_0, h_1, \cdots, h_N\}$.

(2) Calculate the one-step transition probability matrix P using Eq. (26) and Eq. (27).

(3) Determine the initial state probability vector according to the initial PV power generation data by using Eq. (28):

$$P_0 = \begin{bmatrix} P(X_0 = h_1) \\ P(X_0 = h_2) \\ \vdots \\ P(X_0 = h_N) \end{bmatrix},$$
(28)

where $P(X_0 = h_i)$ is the probability that the initial power belongs to h_i.

(4) The state probability matrix P is multiplied by the one-step probability vector of the initial state P_0 to obtain the state probability vector of the power at the forecasted time P_F, shown in Eq. (29).

$$P_F = P \times P_0$$
(29)

(5) Then, the forecasted power P_f^{PV} is obtained by using Eq. (30):

$$P_f^{PV} = P_{EXP} \times P_F,$$
(30)

where P_{EXP} is the average value of each state interval h_i.

B.2 Monte Carlo (MC) forecasting model for EV charging load

Statistical modelling based on the Monte Carlo (MC) simulation is one of the main methods used for EV charging load modelling [64]. The MC charging load forecasting model is based on the charging period [65], which includes the charging characteristics such as the initial charging time, initial SOC of the different types of electric vehicles, and the charging time [66]. Hence, there are two parts in the MC charging load forecasting model; the probabilistic model of the influencing factors and the MC simulation forecasting model.

(1) Probabilistic model of the factors influencing the EV charging process

Types of EVs:

The EVs could be private vehicles, buses, taxis, or official vehicles, according to their purpose. The different types of EVs have different battery and charging characteristics, as well as different charging loads.

Initial charging time:

According to a previous study [66], the initial charging time T_s of the EVs corresponds to the normal distribution $N(\mu_s, \sigma_s^2)$, where μ_s is the expectation and σ_s is the standard deviation.

Initial SOC:

Similarly, according to a previous study [66, 26], the initial SOC s_o corresponds to the normal distribution $N(\mu_o, \sigma_o^2)$ or the average distribution $B(s_{oa}, s_{ob})$, where μ_o is the expectation, σ_o is the standard deviation, s_{oa} and s_{ob} are the residual SOC value boundaries acceptable to the EV users.

Charging time:

The charging time T_c is limited by many factors including temperature, voltage fluctuations, and battery status. For the "based on SOC only" condition, T_c can be formulated as follow, shown in Eq. (31):

$$T_c = \frac{(s_M - s_0)\Theta}{\eta P_{\max}} \quad , \tag{31}$$

where Θ is the EV battery capacity, $P_{\max}$ is the maximum charging power, s_M is the maximum SOC value, the η is the charging efficiency such that, $0.9 \leq \eta \leq 1$.

(2) MC simulation forecasting model for EV charging load

It is assumed that the charging load at time t is the sum of the charging of the single EV in the charging state, which is described by the following dynamic function, shown in Eq. (32)::

$$P_t^{EV} = \sum_i^{N_h} P_{\max}^h + \sum_j^{N_b} P_{\max}^b + \sum_k^{Na} P_{\max}^a + \sum_m^{N_o} P_{\max}^o \, , \tag{32}$$

where N_h, N_b, N_a and N_o are the number of private vehicles, buses, taxis and official vehicles, respectively; P_{max}^h, P_{max}^b, P_{max}^a and P_{max}^o are the corresponding maximum charging power.

First, the MC simulation forecasting model for EV charging load extracts the initial charging time T_s and the initial SOC s_o of each EV by the MC simulation method, to calculate the charging load of each EV. Then, the forecasted value of the total charging load is obtained by stacking all EV charging loads. The simulation calculation flowchart of the EV (using private vehicles as an example) is shown in Fig. 19. The EV battery capacity Θ, the probability distribution of the initial charging time T_s, initial SOC s_o, and the other parameters used in this case study are shown in Table 13. As the scenario in this case study is a charging station in a working area, only private and official vehicles have been considered. The private vehicles are mainly charged during the day, while the official vehicles are mainly charged at night.
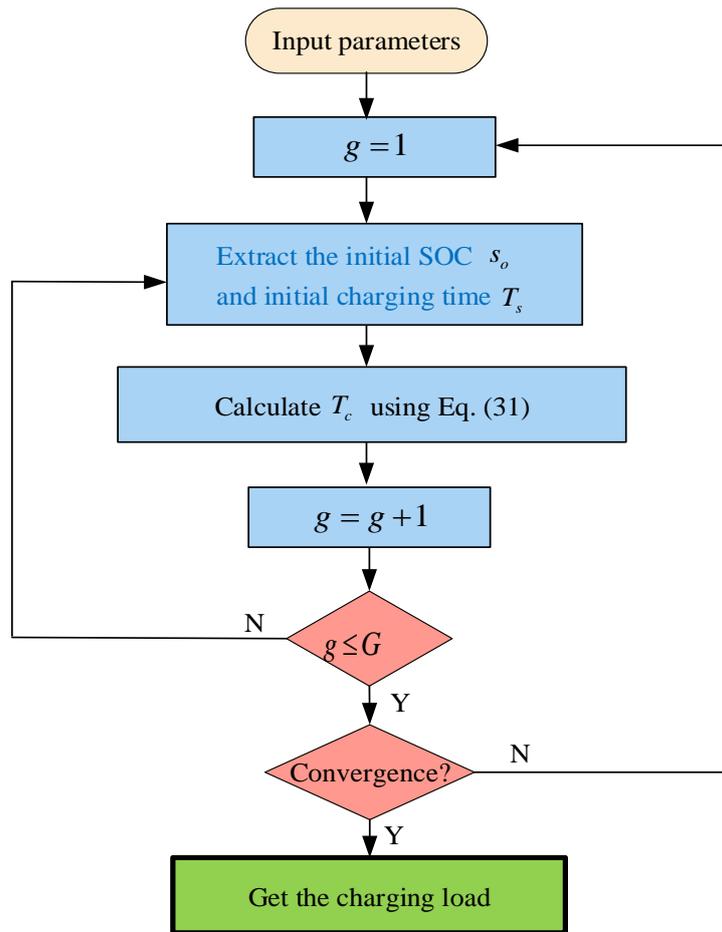

Fig. 19. Flowchart of the MC simulation method for EV charging load

Table 13 MC simulation parameters for EV charging load

EV type	N_h	N_o	Θ	Probability distribution of T_s	Probability distribution of s_o	P^h_{max}	P^h_{max}	s_M	η
Private vehicle	20	-	20 kWh	$N(52,10)$	$B(0.2,0.5)$	5 kWh	-	1	0.95
Official vehicle	-	5	20 kWh	$N(84,6)$	$B(s_{oa},s_{ob})$	-	5 kWh	1	0.95

The coefficient of variance ζ was used to determine the convergence of the MC simulation results, which is defined as follow, shown in Eq. (33):

$$\zeta_i = \frac{\sigma\left(\bar{L}\right)}{\sqrt{g}\,\bar{L}_i},\tag{33}$$

where $\bar{L}_i$ is the charging load expectation at time t, $\sigma\left(\bar{L}\right)$ is the standard deviation at time t, g is the number of calculations, and $\zeta_i = 0.001$ in this case study.

References

[1] Jiang X, Wang J, Han Y, Zhao Q. Coordination dispatch of electric vehicles charging/discharging and renewable energy resources power in microgrid. Procedia Computer Science 2017 107: 157-163.

[2] Zhao J, Wan C, Xu Zh, Wang J. Risk-based day-ahead scheduling of electric vehicle Aggregator using information gap decision in theory. IEEE Transactions on Smart Grid 2017; 8: 1609–1618.

[3] Liu L, Kong F, Liu X, Peng Y, Wang Q. A review on electric vehicles interacting with renewable energy in smart grid. Renewable and Sustainable Energy Reviews 2015; 51: 648-661.

[4] Zhou L, Li F, Gu C, Hu Z, Blond S. Cost/benefit assessment of a smart distribution system with intelligent electric vehicle charging. IEEE Transaction on Smart Grid 2014; 5: 839-847.

[5] Hou H. Xue M, Chen G, Tang J, Xu T, Liu P. Multi-objective hierarchical economic dispatch for microgrid considering charging and discharging of electric vehicles. Automation of Electric Power Systems 2019; 43(17): 55-62.

[6] Shen W, Cui X. Impact of electric vehicles and renewable energy systems on cost and emission of electricity. Proceedings of IEEE 7th Conference on Industrial Electronics and Applications, Singapore, Singapore, 2011: 120-125.

[7] Zhao J, Wen F, Dong Z, Xue Y, Wong KP. Optimal dispatch of electric vehicles and wind power using enhanced particle swarm optimization. IEEE Transaction on Industrial Informatics 2012; 8(4): 889-899.

[8] Chen C, Duan S. Optimal integration of plug-in hybrid electric vehicles in microgrids. IEEE Transaction on Industrial Informatics 2014; 10: 1917-1926.

[9] Ju L, Li H, Zhao J, Chen K, Tan Q, Tan Zh. Multi-objective stochastic scheduling 0ptimization model for connecting a virtual power plant to wind-photovoltaic-electric vehicles considering uncertainties and demand response. Energy Conversion and Management 2016; 128: 160-177.

[10] Yuan G, Wang B. Economic optimal dispatch of virtual power plant with electric vehicles. Acta Energiae Solaris Sinica 2019; 40(8): 2395-2404.

[11] Li Sh, Wu H, Bai X, Yang Sh. Optimal dispatch for PV-assisted charging station of electric vehicles. IEEE PES GTD Grand International Conference and Exposition Asia, Bangkok, Thailand, 2019: 854-859.

[12] Goli P, Shireen W. PV powered smart charging station for PHEVs. Renewable Energy 2014; 66:280-287.

[13] Pinak J, Vincenzo M, Stephen Y, Giorgio R. Economic and environmental impacts of a PV powered workplace parking garage charging station. Applied Energy 2013; 108: 323-332.

[14] Chang F, Huang M, Zhang W. Research on coordinated charging of electric vehicles based on TOU charging price. Power System Technology 2016; 40: 2609-2615.

[15] Francis M, Jackson J, Eun-Kyung Ki, Ton D, Jin-W. Electric vehicles and smart grid interaction: A review on vehicle to grid and renewable energy sources integration. Renewable and Sustainable Energy Reviews 2014; 34: 501-516.

[16] Miloˇs P. Exploitation of electric-drive vehicles in electricity markets. IEEE Transactions on Power Systems 2012; 27: 682-694.

[17] Niklas R., Marija I. Optimal charge control of plug-in hybrid electric vehicles in deregulated electricity markets. IEEE Transactions on Power Systems 2011; 26: 1021-1029.

[18] Ge SH, W ang L, Liu H, Feng L, Haung Ll, Zhu T. An optimization model of peak-valley price time-interval considering vehicle-to-grid. Power System Technology 2013; 37(8): 2316-2321.

[19] Zhang M, Xie Q, Li L, Sun H. Optimal sizing of energy storage for microgrids considering energy management of electric vehicles. Proceedings of the CSEE 2015; 35(18): 4663-4673.

[20] Chen Q, Wang F, Hodge B, Zhang J, Li Zh, Shafie-Khan M, Joao P. Dynamic price vector formation model based automatic demand response strategy for PV-assisted EV charging stations. IEEE Transactions on Power Systems 2017; 8: 2903-2915.

[21] Yeong K, Jeongho K, Song Ch. Dynamic pricing, scheduling, and energy management for profit maximization in PHEV charging stations. IEEE Transactions on Vehicular Technology 2017; 66: 1011-1026.

[22] Yang X, Zhang Y, Jiang Y, Xie L, Zhao B. Renewable energy accommodation-based strategy for electric vehicle considering dynamic interaction in microgrid. Transactions of China Electrotechnical Society 2018; 33(2): 390-400.

[23] Wei W, CHen Y, Liu F, Mei Sh, Tian F, Zhang X. Stackelberg game based retailer pricing scheme and EV charging management in smart residential area. Power System Technology 2015; 39(4): 939-945.

[24] Wang Y, Su Zh, Xu Q, Yang T, Zhang N. A novel charging scheme for electric vehicles with smart communities in vehicular networks. IEEE Transactions on Vehicular Technology 2019; 68: 8487-8501.

[25] Zhang J, Zhang Y, Li T, Jiang L, Li K, Yin H, Ma Ch. A hierarchical distributed energy management for multiple PV-Based EV charging stations. Annual Conference of the IEEE Industrial Electronics Society, Washington, DC, USA, 2018: 1603-1608.

[26] Rui T, H C, Li G, Tao J, Shen W. A distributed charging strategy based on day ahead price model for PV-powered electric vehicle charging station. Applied Soft Computing Journal 2019; 76: 638-648.

[27] Tushar W, Chai B, Yuen C, Smith DB, Wood KL, Yang ZY, Poor HV, Three-party energy management with distributed energy resources in smart grid. IEEE Transaction on Industry Electronics 2015: 62:2487-2498.

[28] Zhang G, Wang X, Jiang Ch. Stackelberg game based coordination dispatch of virtual power plant considering electric vehicle management. Automation of Electric Power System 2018; 42(11): 48-55.

[29] Yang G, Luo H, Wang D, Fu J, Jia R, Yao L. Leader-follower game model of time-of-use electricity price and optimized plug-in electric vehicle dispatching. Proceedings of the CSU-EPSA 2018; 30(10): 55-60.

[30] Zhao T, Li Y, Pan X, Wang P, Zhang J. Real-time optimal energy and reserve management of electric vehicle fast charging station: hierarchical game approach, IEEE Transactions on Smart Grid 2018, 9(5):1-1.

[31] Ma L, Liu N, Zhang J, Tushar W, Yuan Ch. Energy management for joint operation of CHP and PV prosumers inside a grid-connected microgrid: a game theoretic approach. IEEE Transaction on Industrial Informatics 2016; 12(5): 1930-1942.

[32] Ivan V, Marko D, Domagoj J. Improving genetic algorithm performance by population initialisation with dispatching rules. Computers & Industrial Engineering 2019; 137: 1-15.

[33] Feng Zh, Niu W, Cheng C. Optimization of hydropower reservoirs operation balancing generation benefit and ecological requirement with parallel multi-objective genetic algorithm. Energy 2018; 153: 706-718.

[34] Guo H, Bai H, Liu L, Wang Y. Optimal scheduling model of virtual power plant in a unified electricity trading market. Transactions of China Electrotechnical Society 2015; 30(23): 136-145.

[35] Zou S , Ma Z, Liu X, Hiskens I. An efficient game for coordinating electric vehicle charging. IEEE Transactions on Automatic Control 2016; 62(5): 2374-2389.

[36] Ma Z, Yang N, Zou S, Shao Y. Charging coordination of plug-in electric vehicles in distribution networks with capacity constrained feeder lines. IEEE Transactions on Control Systems Technology 2018; 26(5): 1917-1924.

[37] Yu M, Hong S. A real-time demand-response algorithm for smart grids: a Stackelberg game approach. IEEE Transactions on Smart Grid 2016; 7(2):879-888.

[38] Deng X, Guo H. Existence of the equilibrium solution of a two-stage leader-followers game. Mathematics in Economics 2009; 26(4): 50-53.

[39] Liu W, Li X, Liu Z, Wang A, Wang J. Energy operating mode and energy management based on Stackelberg game. Modern Electric Power 2018; 35(2): 8-15.

[40] Wang P, Zou S, Wang X, M Zh. A Stackelberg game approach for price response coordination of thermostatically controlled loads. Applied Sciences 2018; 8: 1-17.

[41] Meng F, Zeng X. A Stackelberg game-theoretic approach to optimal real-time pricing for the smart grid. Soft Computing 2013; 17: 2365-2380.

[42] Maharjan S , Zhu Q , Zhang Y , Gjessing S, Basar T. Dependable demand response management in the smart grid: a Stackelberg game approach. IEEE Transactions on Smart Grid 2013; 4(1):120-132.

[43] Holland J. Adaptation in natural and artificial systems. University of Michigan Press, Ann Arbor, USA, 1975: 515.

[44] Strzalka A, Alam N, Duminil E, Coors V, Eicker U. Large scale integration of photovoltaics in cities. Applied Energy 2012; 93(5): 413–421.

[45] Cheng Q, Zhang Q, Cheng Y, Chu S, Yang X. Short-term photovoltaic power prediction model based on hierarchical clustering of density peaks algorithm. High Voltage Engineering 2017; 43(4): 1214-1222.

[46] Utpal D, Kok T, Mehdi S, Saad M, Ben H, Alex S. SVR-based model to forecast PV power generation under different weather conditions. Energies 2017, 10(7):876.

[47] Zhao W, Dai T, Wang L, Ke L. Short-term load forecasting considering meteorological factors and electric vehicles. IOP Conference Series Materials Science and Engineering 2018; 439: 032114.

[48] Li Y, Davis C, Lukszo Z, Weijnen M. Electric vehicle charging in China's power system: energy, economic and environmental trade-offs and policy implications. Applied Energy 2016; 173: 535–54.

[49] Arias M, Bae S. Electric vehicle charging demand forecasting model based on big data technologies. Applied Energy 2016: 183:327-339.

[50] Xydas E, Marmaras C, Cipcigan L, Jenkins N, Carroll S. A data-driven approach for characterising the charging demand of electric vehicles: A UK case study. Applied Energy 2016; 162:763-771.

[51] Liu L, Zhao Y, Sun Q, Wennersten R. Prediction of short-term output of photovoltaic system based on generalized regression neural network. IEEE Conference on Energy Internet and Energy System Integration, Beijing, China, 2017: 1-6.

[52] Wang X, Huang K, Zheng Y, Li L, Shao F, Jia L, Xu QS. Combined PV power forecast based on firefly algorithm-generalized regression neural network. Power System Technology 2017; 41(2): 455-461.

[53] Liu L, Zhao Y, Chang D, Xie J, Ma Zh, Qie S, Yin H, Wennersten R. Prediction of short-term PV power output and uncertainty analysis. Applied energy 2018; 228: 700-711.

[54] Mandal P, Haque A, Madhira S, Al-Hakeem D. Applying wavelets to predict solar PV output power using generalized regression neural network. North American Power Symposium, Manhattan, USA, 2013: 1-5.

[55] Dong L, Wang L, Khahro S, Gao S, Liao X. Wind power day-ahead prediction with cluster analysis of NWP. Renewable and Sustainable Energy Reviews 2016; 60: 1206-1212.

[56] Azimi R, Ghofrani M, Ghayekhloo M. A hybrid wind power forecasting model based on data mining and wavelets analysis. Energy Conversion and Management 2016; 127: 208-225

[57] Hao Y, Dong L, Liao X, Liang J, Wang L. A novel clustering algorithm based on mathematical morphology for wind power generation prediction. Renewable Energy 2019; 136: 572-585.

[58] Samina K, Xu H, Iftikhar H,Zhu W, Misha Z. Integration of data mining clustering approach in the personalized E-learning system. IEEE Access 2018; 6: 72724-72734.

[59] Xie J, Qu Y. K-medoids clustering algorithms with optimized initial by density peaks. Journal of Frontiers of Computer Science and Technology 2016; 10(2): 230-247.

[60] Gao S, Dong L, Tian Ch, Liao X. Wind Power Prediction Using Time-Series Analysis Base on Rough Sets. International Conference on Electric Information and Control Engineering, Wuhan, China, 2011: 2847-2852.

[61] Louie H. Time series modeling of aggregated electric vehicle charging station load. Electric Power Components and System 2017; 45(14): 1498-1511.

[62] Li Y, He L, Niu J. Forecasting power generation of grid-connected solar PV system based on Markov chain. Acta Energiae Solaris Sinica 2014; 35(4): 611-616.

[63] Ding K, Feng L, Wang X, Qin S. Forecast of PV power generation based on residual correction of Markov chain. International Conference on Control, Automation and Information Sciences, Changshu, China, 2015:355-359.

[64] Li H, D Z, Chen L, Guan S, Zhou B. Trip simulation based charging load forecasting model and vehicle-to-grid evaluation of electric vehicles. Automation of Electric Power System 2019; 43(21): 88-96.

[65] Wang H, Zhang Y, Mao H. Load forecasting method of EVs based on time charging probability. International Conference on Power System Technology, Guangzhou, China, 2018: 1731-1735.

[66] Chen L, Zhang Y. Research on load forecasting system for electric vehicle charging. Journal of electric Power Science and Technology 2014; 29(1): 29-36.